Tomas Bata University in Zlín
Library

Hierarchy of nanoparticles toxicity factors significance as extracted from NanoCommons knowledge base: influence of compound, cell line and particle size on cell viability

Citation

MACKO, Michal, František BOŽEK, Diana KMEŤKOVÁ, Jan ANTOŠ, and Ivo KUŘITKA. Hierarchy of nanoparticles toxicity factors significance as extracted from NanoCommons knowledge base: influence of compound, cell line and particle size on cell viability. *Nanotoxicology* [online]. vol. 19, iss. 6, Taylor & Francis, 2025, p. 553 - 574 [cit. 2026-10-05]. ISSN 1743-5390. Available at https://www.tandfonline.com/doi/full/10.1080/17435390.2025.2555307

DOI

https://doi.org/10.1080/17435390.2025.2555307

Permanent link

https://publikace.k.utb.cz/handle/10563/1012647

This document is the Accepted Manuscipt version of the article that can be shared via institutional repository.

TBU Publications
Repository of TBU Publications
publikace.k.utb.cz

Hierarchy of nanoparticles toxicity factors significance as extracted from NanoCommons knowledge base: influence of compound, cell line and particle size on cell viability

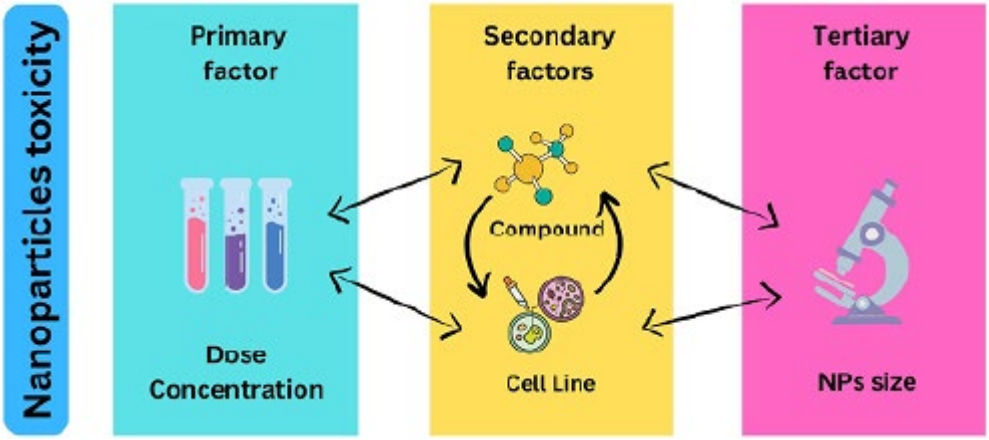
Michal Macko[a,*], František Božek[a], Diana Kmeťková[b], Jan Antoš[a], Ivo Kuřitka[a,*]

[a]*Centre of Polymer Systems, Tomas Bata University in Zlín, Zlín, Czech Republic*
[b]*Institute of Economic Studies, Charles University, Prague, Czech Republic*

*Corresponding author: kuritka@utb.cz, mmacko@utb.cz

ABSTRACT

The objective of the paper was to conduct a thorough statistical meta-analysis of a publicly available database by examining cell membrane damage (CMD), mitochondrial membrane potential (MMP), nuclear size (NS), nuclear intensity (NI), and cell viability (CVV) responses toward nanoparticles. The set of individual 880 and the subset of 630 measurements contained exposure dose, particle diameter, nanoparticle identity (TiO_2, Ag, SiO_2, CeO_2, ZnO, Cu), and cell type (A549, HCT116, HepaRG, HEPG2, RAW264.7) correlated to toxicity markers. The exposure dose was revealed as the most consistent predictor of toxicity across all endpoints, with higher doses significantly influencing toxicity. The compound-specific response was another important factor, where Ag, ZnO, and Cu, were consistently more cytotoxic, while ZnO and Cu correlated to loss of CVV and MMP. Contrary, TiO_2, CeO_2 and SiO_2 displayed partial protective effects, depending on cell context. The effect of particle size was compound- and endpoint-specific, e.g. smaller particles of CeO_2 displayed greater disruption to nuclear architecture (NS, NI) and MMP, while size had minimal effect on CVV for other compounds. HepaRG cells were the most sensitive, specifically from Cu and ZnO, while epithelial lines (e.g. HCT116, HEPG2) showed more complex patterns. Generally, the dose was confirmed as the most impactful predictor, due to consistent and statistically significant effects. Compounds and cell lines were determined as factors of next-highest importance, displaying mixed but significant effects, and the particle size showed lowest effects. These findings highlight the importance of multi-endpoint, multi-cell-type frameworks in nanotoxicology for compound- and cell-specific risk assessments.



KEYWORDS: Nanoparticles, toxicity, statistical analysis, particle size

Introduction

Nanoparticles (NPs) are defined as particles with at least one dimension ranging between 1 - 100 nm (**Bezza, Tichapondwa, and Chirwa 2020**). Some studies may include particles that slightly exceed the formal nanoscale limit, as long as they demonstrate properties or phenomena typically associated with the nanoscale. Their properties, emerging due to their small size and high surface-to-volume ratio, are explored in many industrial fields, such as medicine (**Islam et al. 2022**), electronics (**Chakraborty et al. 2022**), agriculture (**ESKİN 2022; Pansambal et al. 2023**) or environmental science (**Arun et al. 2023; Samuel et al. 2022**). Besides their positive properties, they also have adverse toxicological effects on biological systems (**Gupta and Xie 2018**). Therefore, the mechanisms of nanoparticle-induced toxicity are intensively researched (**Gudkov et al. 2021; Naz, Gul, and Zia 2020; Nie, Zhao, and Xu 2023; Thakur et al. 2024**). The toxicity mechanisms depend on numerous factors, while the most acknowledged are elemental composition, size, shape, or surface charge (**Abbasi et al. 2023**). A large amount of knowledge has been gathered but remains dispersed among individual studies. To obtain the bird's-eye view on the multiple sources of various data, an H2020 Infrastructures project, NanoCommons was executed creating a community framework and infrastructure for reproducible science, and in particular for in silico workflows for nanomaterials safety assessment and beyond (**NanoCommons: The European Nanotechnology Knowledge Infrastructure 2025**). The NanoCommons provides a knowledge base in a form of database, containing reliable and concise data on nanoparticle characterization and toxicity, intended to improve access to and quality of nano informatics in Europe.

Compounds

This paper examines the toxicological behavior and mechanisms of toxicity of six commonly used compounds in nanoparticle (NP) form, extracted from the NanoCommons database. These include: (i) oxide materials - titanium dioxide (TiO_2), zinc oxide (ZnO), cerium dioxide (CeO_2), and silicon dioxide (SiO_2); and (ii) metals - silver (Ag) and copper (Cu).

Titanium dioxide (TiO_2)

Titanium dioxide (TiO_2) is one of the most widely produced semiconducting nanomaterial. $TiO_2\ NPs$ possess UV-blocking and photocatalytic properties, high stability, and biocompatibility. Although $TiO_2\ NPs$ are generally considered biologically inert under dark conditions, upon photoactivation by UV light, they generate reactive oxygen species (ROS), can cause DNA damage, or lead to pulmonary toxicity after inhalation (**Mohamed 2015; Ziental et al. 2020**). Another factor influencing the toxicity of $TiO_2\ NPs$ is the crystal structure - anatase vs. rutile. The observations indicate that the anatase form is more toxic due to higher photocatalytic activity leading to increased generation of ROS (**Baranowska-Wójcik et al. 2020; Nosaka and Nosaka 2017; Thakur et al. 2024**).

Zinc dioxide (ZnO_2)

Zinc oxide nanoparticles ($ZnO\ NPs$) are also mass-scale produced and have already been introduced in many applications utilizing their antimicrobial and UV protective functions and relatively high biocompatibility. Interestingly, enhancement of drug delivery was also reported. (**Gudkov et al. 2021; Islam et al. 2022; Silva et al. 2019**). On the other hand, $ZnO\ NPs$ can cause oxidative stress, lipid peroxidation, DNA damage, and ultimately, cell death, which are ascribed to the formation of reactive

oxygen species (ROS) or due to the release of zinc ions (Zn^{2+}) (**Canta and Cauda 2020; Chang et al. 2012; Chen et al. 2019; Fukui et al. 2012; Song et al. 2010**).

Cerium dioxide (CeO_2)

Another industrial large-scale produced semiconductor nanomaterial is cerium dioxide (CeO_2). CeO_2 NPs can act both as antioxidants and prooxidants, due to their ability to switch between cerium (III) and cerium (IV) oxidation states, often used as catalyst. The nature of CeO_2 NPs allows to scavenge ROS and protect cells from oxidative damage continuously (**Singh et al. 2020**), and for that reason, among many others, their applications can be found in sunscreens or cosmetics. (**Pansambal et al. 2023**). Nevertheless, at higher concentrations, CeO_2 NPs can induce oxidative stress, cause DNA damage, or trigger immune responses and inflammation (**Forest et al. 2017; Gao et al. 2014**).

Silicon dioxide (SiO_2)

Silica, i.e. silicon dioxide (SiO_2) nanoparticles, is the second most widely produced oxide nanomaterial after alumina. SiO_2 NPs are widely used in food, cosmetics, and pharmaceuticals because of their biocompatible and chemically stable properties (**Slowing et al. 2008**). While generally recognized as considerably less toxic than other nanoparticles, SiO_2 NPs can induce toxicity associated with surface reactivity, which can lead to the generation of ROS, inflammatory responses, membrane damage, and DNA fragmentation (**El-Sayed, El-Demerdash, and El-Magd 2021; ESKİN 2022; Liman et al. 2020; Rafieepour et al. 2021; Yang et al. 2019**).

Silver nanoparticles (Ag)

Due to their exceptional antimicrobial and biocompatible properties, metal silver nanoparticles (Ag NPs) are used in many fields such as agriculture, electronics, textile, hygiene or medicine and medical devices. When it comes to the mechanism of toxicity, primarily, it is the release of silver ions (Ag^+) that induces oxidative stress. Direct nanoparticle interaction with the cell membrane was also described. Next, even in the absence of ROS, Ag NPs can cause damage to the mitochondrial function, leading to the cell death (**Bruna et al. 2021; Luceri et al. 2023; Nie, Zhao, and Xu 2023; Xu et al. 2020**).

Copper oxide (CuO)

Another widespread material is copper (Cu) and copper-based NPs, often in the form of metal oxide (CuO). Among others, metal Cu NPs are used as materials for superconductors in electronics or as antimicrobial agents for coatings and food preservatives (**Chakraborty et al. 2022; Naika et al. 2015; Yip and Sauls 1992**). However, when they interact with biological systems, copper ions (Cu^{2+}) may be released, which may induce oxidative stress, or cause mitochondrial malfunction and DNA damage (**Ahamed et al. 2010; Akintelu et al. 2020; Fahmy and Cormier 2009; Naz, Gul, and Zia 2020**).

Cell lines

Understanding the toxic potential of nanoparticles requires also careful consideration of their biological targets. The target is determined by the method used - $in\ vitro$ (outside of a living organism)

or $in\ vivo$ (within a living organism) (**Savage, Hilt, and Dziubla 2019**). The scope of this paper focuses on in vitro methods, specifically measurements conducted on cell lines. Each cell line used for testing represents specific tissue characteristics, metabolic capacities, and stress response mechanisms, resulting in their different sensitivity to various compounds. Therefore, selecting appropriate cell lines is critical for understanding toxicity mechanisms, predicting in vivo responses, and evaluating potential risks (**Kumar, Sharma, and Maitra 2017**). Among the cell lines examined in the studies collected in the NanoCommons database, five cell lines are relevant in this study, namely HepG2, HepaRG, A549, RAW264.7, and HCT116. This selection covers four important areas of human organism toxicity, i.e., toxicity to the liver, gastrointestinal tract, pulmonary system, and inflammation responses.

HepG2 - human hepatocellular carcinoma cell line

The widely used model for hepatic metabolism and cytotoxicity studies are $HepG2$ cells which are derived from human liver carcinoma (**Ahamed, Akhtar, and Alhadlaq 2020; Elje et al. 2020; Yuan et al. 2011**). In particular, HepG2 cells are relevant for studying effects of nanoparticles that release metal ions when dissolving, such as ZnO, TiO_2, Ag or Cu, due to their role in metabolizing reactive compounds and detoxifying oxidative stress (**Brandão et al. 2020; Brkić Ahmed et al. 2017; Liu et al. 2021; Reihani, Shaki, and Azari 2025**).

HepaRG - human hepatic progenitor cell line

Compared to HepG2, $HepaRG$ (Human Hepatocellular cells) are considered a superior model for studying hepatotoxicity (**Guo et al. 2020**). It is due to their ability to replicate the metabolic and inflammatory responses of liver cells in the human body toward various compounds, including NPs. Furthermore, their sensitivity to oxidative stress and metal ions makes them an ideal model used for distinguishing between direct cytotoxic effects and metabolism-dependent toxicity (**Helvenstein et al. 2015; Kuhn et al. 2024; Voss et al. 2020**).

HCT116 - human colorectal carcinoma cell line

The response of gastrointestinal tract is modeled by $HCT116$ cell line which is derived from human colorectal carcinoma. HCT116 cells are often used to study the gastrointestinal toxicity of nanoparticles, particularly those administered orally or exposed via dietary sources. These cells are highly proliferative and exhibit strong DNA repair mechanisms, which make them a robust model for studying genotoxicity and oxidative stress (**Ahmed et al. 2015; Gurunathan et al. 2018; Jia et al. 2020; Vecchiotti et al. 2021**).

A549 - human alveolar basal epithelial cell line

A commonly used model for respiratory toxicity is $A549$ cells, which are derived from human alveolar basal epithelial cells (**Ahamed, Akhtar, and Alhadlaq 2019; Ahmad et al. 2018**). A unique feature of A549 cells is their suitability for testing the particle size-dependent uptake and cytotoxicity, which is due to the larger nanoparticles remaining in the extracellular space, while smaller particles are translocated deeper and absorbed by cells (**Chairuangkitti et al. 2013; Kim et al. 2006; Rafieepour, Azari, and Khodagholi 2023**).

RAW264.7 - Murine macrophage-like cell line

The model frequently used to investigate how the immune system reacts to nanoparticles are $RAW264.7$ cells, derived from murine macrophages. Besides their origin, it is due to their ability to produce high level of ROS when exposed to foreign substances (**Bo et al. 2023**). For that reason, they are recognized as a valuable model for researching inflammation and oxidative stress brought on by nanoparticles (**Dussert et al. 2020; Giovanni et al. 2015; Hsieh et al. 2015**).

Toxicity response indicators

The last piece of information is how toxicity is determined for given compound on given cell line. In this paper, focus it set on five toxicity markers, that were also available in the NanoCommons knowledge base, specifically - Cell membrane damage (CMD), Mitochondrial membrane potential (MMP), Nuclear intensity (NI), Nuclear size (NS) and Cell viability (CVV).

All these markers play a crucial role when evaluating toxicity, based on their collective ability to capture diverse structural, functional, and metabolic changes in cells exposed to toxic compounds. The connection of these markers, in a very simple terms, can be described in a logical flow: once cell experiences stress or is exposed to foreign (toxic) substance, it damages cell membrane and mitochondria, which leads to disruption of adenosine triphosphate (ATP) and cellular homeostasis, leading to nuclear morphology changes (size and intensity), that eventually might lead into loss of cell viability (**Riss et al. 2013**).

$Cell\ membrane\ damage$ (CMD) reflects the physical integrity of the plasma membrane. Its disruption is a sign of necrosis and terminal apoptosis, indicating irreversible loss of cell viability (**Vijayaraghavareddy et al. 2017**). $Mitochondrial\ membrane\ potential$ ($\Delta\psi m$) (MMP) represents mitochondrial health and energy production. A reduction in ($\Delta\psi m$ is often one of the earliest signs of cellular stress and apoptosis initiation (**Zorova et al. 2018**). $Nuclear\ intensity$ (NI) highlights chromatin condensation and DNA fragmentation—both characteristic features of apoptotic cell death. It allows for early detection of nuclear responses to toxic stimuli and $nuclear\ size$ (NS) provides structural insights into changes in nuclear morphology. Reduction often marks apoptotic shrinkage, while enlargement may suggest polyploidy, senescence, or mitotic failure (**Belhadj et al. 2023; Mukherjee Chen, and Levy 2016**).

$Cell\ viability$ serves as the integrative endpoint, quantifying the proportion of live versus dead cells. Viability assays provide a high-level readout of cellular health and correlate with metabolic function, proliferation, or membrane integrity depending on the assay used (**Riss et al. 2013**).

Mechanistic Interrelationship between toxicity markers

The five above-mentioned endpoints reflect different but interconnected aspects of cellular health. Although these parameters can be analyzed independently, toxicological processes often involve a cascade of events that are interlinked. Based on this theoretical foundation, it is feasible to construct a mechanistic pathway - whether apoptotic, necrotic, or mixed in nature. The assumed mechanistic interrelationship between observed toxicity markers is displayed in **Figure 1** (**Belhadj et al. 2023; Riss et al. 2013; Mukherjee Chen and Levy 2016; Vijayaraghavareddy et al. 2017; Zorova et al. 2018**).

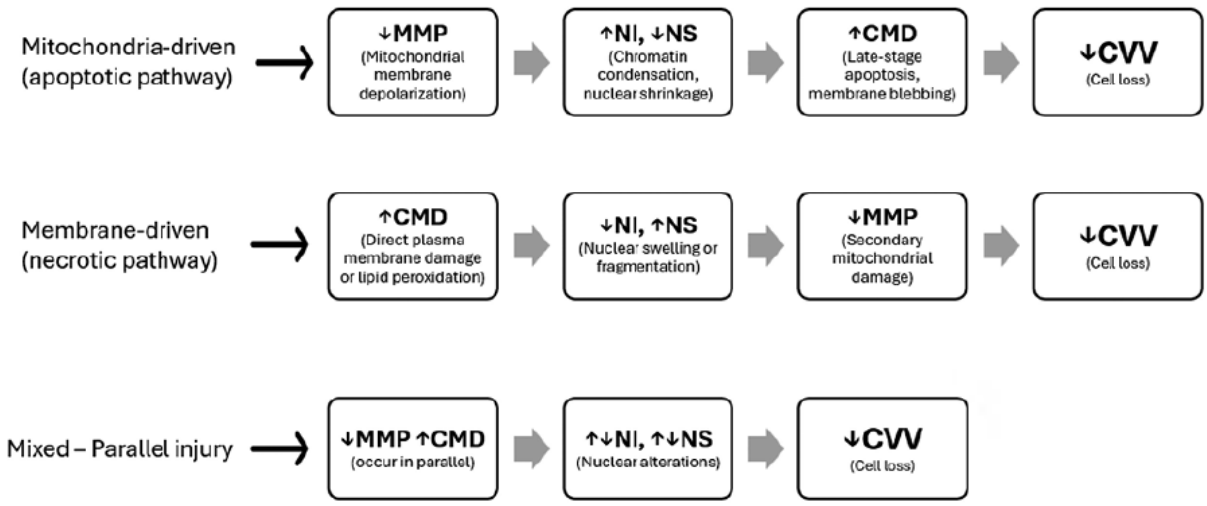


Figure 1. Assumed mechanistic Interrelationship between toxicity markers.

Study purpose

Following on the abovementioned theoretical foundation, the paper will focus on in-depth analysis on how nanoparticle characteristics - especially particle diameter - influence cell viability, and moreover, on how different partial toxicity markers predict the overall toxicity outcome in terms of cell viability. Namely, nuclear size, nuclear intensity, cell membrane potential and mitochondrial membrane potential will be investigated, leveraging the NanoCommons database. This approach not only contributes to the ongoing efforts of safe-by-design nanoparticle development but also provides evidence-based guidance for nanotoxicological risk assessment.

Data and methods

This work aimed to subject the publicly accessible dataset from the NanoCommons database (available under Creative Commons Attribution 4.0 International (CC BY 4.0)) to statistical analysis to verify how different parameters, specifically nanoparticle diameter, nanoparticle composition, and testing method influenced toxicity scores. It is important to state, that this presents significant limitation of study as it focuses solely on export from the database. On the other hand, it ensures that data are consistent, relevant and reliable for purposes of statistical analysis.

The whole database contains a total of 1,630 different measurements, from three leading independent research institutions, 12 different examined compounds, and six different cell lines. After closer examination it became visible that not all observations are containing all necessary information, and it was required to refine the data. The requirements for the purpose of analysis as follows:

1. Each measurement was required to contain
    a. Compound
    b. Exposed cell
    c. Exposure time
    d. Exposure dose
    e. Particle diameter
    f. CMD, MMP, NI, NS, CVV value

7. Each compound was required to contain
    a. Multiple different cell lines
    b. Multiple exposure doses
    c. Multiple particle diameters

Another finding from the dataset is that the exact type of cell viability assay (e.g., MTT, WST-1, resazurin, etc.) is not specified. Although different assays measure cell viability through distinct mechanisms, they all serve to indicate a reduction in viable cells upon toxic exposure (**Single et al. 2015**). For the purpose of this analysis, cell viability is interpreted as a normalized proxy of cytotoxic response, independent of the exact assay. This simplification enables comparative analysis of nanoparticle effects on cell lines and particle characteristics.

Finally, if the measurement was not meeting above-mentioned requirements, it was excluded from the analysis. The final version of used variables is displayed in **Table 1**, where it was possible to preserve 880 measurements in total (54% coverage from the original dataset) for the analysis of CVV, and from these 880, it was possible to preserve 630 measurements (39% coverage from the original dataset) for the analysis of other toxicity markers. The resulting coverage displays the complexity of the topic and difficulty of data compilation from various sources. Such great data reduction is needed to mitigate data misinterpretation due to gaps in the dataset. The complete data set is attached in the supplementary data of the paper.

Table 1. List of parameters available in NanoCommons database.

Parameter	Values present for given parameter
Compounds	880
ExposedCell	880
ExposureTime (h)	880
ExposureDosis [µg/ml]	880
ParticleDiameter [nm]	880
ViableCellCount (%)	880
CellMembraneDamage	630
Mitochondrial membrane potential	630
NuclearIntensity	630
NuclearSize	630

Statistical analysis

The statistical analysis was performed in R-Studio. Plots were generated with the ggplot2 package, and an interactive chart was created using the Plotly package. Multiple Ordinary Least Squares (OLS) regression was employed to analyze the data. This statistical technique estimates the coefficients of the linear relationship between the dependent variable and several independent variables by minimizing the sum of the squared differences between the observed and predicted values. In this paper, the relationship between cell viability and multiple regressors, such as dose, particle diameter, compound, and cell line was modeled.

For this analysis, two different model specifications were explored. The first was a Multiple OLS Model without interactions (Model 1), aimed at exploring the significance of certain variables and their effect on cell viability without considering any interactions. The second was a Multiple OLS Model with

interactions (Model 2), which aimed to explore the significance of certain variables on cell viability while also considering interactions between some of the regressors.

The structural form of Model 1 was defined by Formula 1:

$$\begin{aligned} Cell\,Viability = {} & \beta_0 + \beta_1\left(\log\left(Dose\right)\right) + \beta_2\left(Particle\,Diameter\right) \\ & + \beta_3\left(Compound\right) + \beta_4\left(Cell\,line\right) + \epsilon \end{aligned} \tag{1}$$

Explanation of the Terms applicable for Formula 1:

- β_0: The intercept, representing cell viability when all independent variables are at their baseline values.
- β_1: The coefficient for the logarithmic exposure dose, showing how relative changes in the dose affect cell viability.
- β_2: The coefficient for particle diameter, indicating the effect of nanoparticle size on cell viability.
- β_3: The coefficient for the compound variable. Since $compound$ is a categorical variable, β_3 denotes a vector of estimates (for particular compounds).
- β_4: The coefficient for the exposed cell line variable. Similarly to β_3, it is a vector of coefficients.
- $\in$: The error term, capturing variability not explained by the model.

The structural form of Model 2 was as follows:

$$\begin{aligned} Cell\,Viability = {} & \beta_0 + \beta_1\left(\log\left(Dose\right)\right) + \beta_2\left(Particle\,Diameter\right) \\ & + \beta_3\left(Compound\right) + \beta_4\left(Cell\,line\right) \\ & + \beta_5\left(Particle\,Diameter\right) \times \left(Compound\right) + \epsilon \end{aligned} \tag{2}$$

The difference between Model 1 (without interactions) and Model 2 (with interactions) was the addition of the interaction term between particle diameter and compounds. This enabled examination whether the effect of particle diameter was dependent on the compound or not.

Besides that, the sensitivity analyses were conducted, by sub-setting the final sample. First, the relationship between the independent variables and cell viability by compounds was explored. The goal was to investigate whether the significance (and the direction of the effect) of the dose and particle diameter (when applicable) stayed the same as in the full model. The structural equation for the Multiple OLS model by compounds was as follows:

$$\begin{aligned} Cell\,Viability_i = {} & \beta_0 + \beta_1\left(\log\left(Dose_i\right)\right) + \beta_2\left(Particle\,Diameter_i\right) \\ & + \beta_3\left(Cell\,line_i\right) + \epsilon_i \end{aligned} \tag{3}$$

where $i = 1, \ldots, N$.

Second, the sample was divided based on the cell lines. The structural equation for Multiple OLS model by cell lines was as follows:

$$Cell\,Viability_i = \beta_0 + \beta_1\left(\log\left(Dose_i\right)\right) + \beta_2\left(Particle\,Diameter_i\right) + \beta_3\left(Compounds_i\right) + \epsilon_i \quad (4)$$

where $i = 1,\ldots,N$.

Explanation of the Terms applicable for Formulas 3 & 4:

- β_0: The intercept, representing cell viability when all independent variables are at their baseline values.
- β_1: The coefficient for the logarithmic exposure dose, showing how relative changes in the dose affect cell viability.
- β_2: The coefficient for particle diameter, indicating the effect of nanoparticle size on cell viability.
- β_3: The coefficient for the cell line (Formula 3) or compound variable (Formula 4).
- ϵ_i: The error term, capturing variability not explained by the model.

Results

The refined database can be found in the supplementary documents of this paper, and the 880 measurements from seven datasets contained five cell lines and six compounds, and their combinations is displayed in **Table 2**.

Subsequently, the exposure doses ranged from 0.3 to 250 [μg/ml], and the particle diameters ranged from 8 to 150 nm, as displayed in **Table 3**. Interestingly, toxicity markers contained both positive and negative values, which can be attributed to less toxic results compared to the control sample.

Additionally, the exposure time was constant for all measurements - 24h, as per NanoCommons database. This helped to maintain comparability of different exposure concentrations which reflected the biologically relevant or reported ranges for each cell line-compound combination.

Table 2. Compounds vs. exposed cell line counts.

ExposedCells/ Compounds	A549	HCT116	HepaRG	HEPG2	RAW264.7
Ag	16	16	50	16	16
CeO_2	16	16	20	16	16
Cu	0	0	20	0	0
SiO_2	24	24	170	24	24
TiO_2	48	48	100	48	48
ZnO	16	16	40	16	16

Table 3. Summary statistics of continuous variables used in the model.

Statistic	Min	Mean	Median	Max	Std Dev
ExposureDosis [µg/ml]	0,30	33,85	7,80	250,00	58,49
ParticleDiameter [nm]	8,00	39,86	20,00	150,00	43,55
ViableCellCount	−26,98	−2,02	−0,64	2,43	4,38
CellMembraneDamage	−8,11	11,09	0,55	538,58	44,99
_data.Mitochondrial membrane potential. Value	−14,76	−1,11	−0,58	10,52	2,90
NuclearIntensity	−11,77	1,32	0,20	38,47	4,21
NuclearSize	−35,43	0,50	0,19	49,02	4,26
ExposureTime	24.00	24.00	24.00	24.00	0.00

Multiple OLS model (cell viability - with and without interactions)

The aim was to explore the significance of variables on cell viability variable (CVV), displayed in **Table 4**. The base for the analysis was Ag nanoparticles for compounds, and A549 for cell lines, and these two variables are displayed in the table under $Constant$. The results in each column for Model 1 and Model 2 are displaying difference of the effect of other nanoparticles compared to the effect of Ag nanoparticles, and the effect of other cell lines compared to the effect of A549 cell line on cell viability. In Model 1, the analysis focused solely on the raw effect of compounds on cell viability compared to Ag nanoparticles, while in Model 2, the analysis was extended and considered also size of nanoparticles.

The first variable, $log(ExposureDosis)$, was negative and statistically significant for both models, having the same value (-1.002). A 100% increase in the exposure dose was associated with approximately a 1 percentage point decrease in CVV.

Results for compounds highlight the varying effect of each compound in comparison to the base compound, which was Ag. Compared to Ag, CeO_2, SiO_2, and TiO_2 had a positive and significant effect. On the other hand, Cu and ZnO resulted in a strong negative effect, indicating a substantial reduction in cell viability compared to Ag. Interestingly, results for ZnO nanoparticles in Model 1 are significant (compared to Ag, ZnO is associated with a 2.369 percentage point decrease in CVV), whereas in Model 2, which contains the interaction with particle diameter, the estimates are not significant.

For cell lines, the results were stable across both models in terms of significance and values. HCT116 and HepaRG cells displayed a negative effect on CVV and were statistically significant, while HEPG2 and RAW264.7 displayed a positive effect on CVV but lacked statistical significance, raising questions about the resilience (sensitivity) of specific cell lines to different compounds.

The variable $ParticleDiameter$ had a statistically significant positive effect ($p < 0.05$) in the model without interactions. However, in the model with interactions, the effect of the diameter and compounds became more complex, as the direct effect was not immediately apparent.

We can derive the effect of diameter on CVV by taking the first derivative of CVV with respect to diameter (from **Equation 2**). The derivative is equal to $\beta_2 + \beta_5$*Compound, hence, the effect of diameter is now dependent on the compound. For Ag, the effect of diameter is exactly β_2, but this estimate is not significant. In contrast, diameter appears to play a role for Cu compounds. Increasing the diameter by 1 (or 10) nm is linked to a 0.776 (7.76) percentage point increase in CVV for Cu compared to Ag.

Table 4. Results of model with and without interactions.

	Dependent variable:	
	Viable cell count	
	Model 1	Model 2
	(1)	(2)
log(ExposureDosis)	−1.002***	−1.002***
	(0.063)	(0.063)
ParticleDiameter	0.011*	0.003
	(0.006)	(0.036)
CompoundsCeO_2	3.094***	4.610***
	(0.482)	(1.740)
CompoundsCu	−5.821***	−14.424***
	(0.823)	(2.953)
CompoundsSiO_2	3.215***	2.867***
	(0.382)	(0.915)
CompoundsTiO_2	2.494***	2.417***
	(0.369)	(0.893)
CompoundsZnO	−2.369***	3.408
	(0.854)	(9.477)
ExposedCellHCT116	−0.823*	−0.823*
	(0.430)	(0.428)
ExposedCellHepaRG	−1.330***	−1.371***
	(0.365)	(0.367)
ExposedCellHEPG2	0.980**	0.980**
	(0.436)	(0.435)
ExposedCellRAW264.7	0.608	0.608
	(0.436)	(0.435)
ParticleDiameter:CompoundsCeO_2		−0.056
		(0.066)
ParticleDiameter:CompoundsCu		0.776***
		(0.250)
ParticleDiameter:CompoundsSiO_2		0.013
		(0.036)
ParticleDiameter:CompoundsTiO_2		0.003
		(0.037)
ParticleDiameter:CompoundsZnO		−0.033
		(0.074)
Constant	−1.556***	−1.362
	(0.444)	(0.891)
Observations	880	880
R^2	0.429	0.437
Adjusted R^2	0.422	0.426
Residual std. error	3.331 (df = 868)	3.317 (df = 863)
F statistic	59.266*** (df = 11; 868)	41.842*** (df = 16; 863)

Note: $^{*}p < 0.1$; $^{**}p < 0.05$; $^{***}p < 0.01$.

Analogically, we can analyze the difference between Ag and the other compounds. By taking the first derivative of CVV with respect to the compound, we get $\beta_3 + \beta_5$*Diameter. If the diameter was 0, there is no interaction effect and the effect of a compound on the outcome is exactly the respective estimate of β_3. However, the minimum value of diameter is 8 nm, meaning that the interaction term is taken into account. Particularly, the effect of Cu on CVV depends on the particle diameter as the interaction was significant. In other words, the effect of Cu on CVV can be computed as -14.424+0.776*diameter. As the particle diameter increases, the effect of Cu on CVV (compared to Ag) becomes less negative. If the diameter is 1 nm, the effect of Cu on CVV (compared to Ag and holding other variables constant) is -13.359. If the diameter is 10 nm, Cu would be associated with a 6.664 percentage point decrease in CVV compared to Ag.

Multiple OLS model (cell viability by compounds)

The aim was to explore how specific factors influence CVV separately for each compound (decreasing the sample size compared to the whole-sample regression) and whether these effects are consistent with the whole-sample results. The base ($Constant$) for cell lines was A549, which was selected to compare the effect of other cell lines on cell viability, and the results are displayed in **Table 5** below.

Table 5. Results of multiple OLS model by compounds.

	Dependent variable:					
	Viable Cell Count					
	TiO_2	Ag	SiO_2	CeO_2	ZnO	Cu
	(1)	(2)	(3)	(4)	(5)	(6)
log(ExposureDosis)	−0.759***	−1.697***	−0.289***	−0.122***	−3.067***	−3.136***
	(0.086)	(0.162)	(0.048)	(0.040)	(0.273)	(0.547)
ParticleDiameter	0.005	−0.006	0.010***	−0.053***	−0.030	0.779**
	(0.007)	(0.034)	(0.004)	(0.010)	(0.096)	(0.362)
ExposedCellHCT116	−0.525	2.079*	−0.475	−0.202	−5.764***	
	(0.517)	(1.082)	(0.422)	(0.221)	(1.723)	
ExposedCellHepaRG	−2.418***	2.519***	−1.853***	−0.736***	−1.972	
	(0.458)	(0.916)	(0.335)	(0.215)	(1.477)	
ExposedCellHEPG2	−0.227	5.956***	−1.047**	−0.506**	4.246**	
	(0.527)	(1.099)	(0.425)	(0.226)	(1.753)	
ExposedCellRAW264.7	0.032	4.392***	−1.339***	−0.860***	3.033*	
	(0.527)	(1.099)	(0.425)	(0.226)	(1.753)	
Constant	1.194***	−3.059***	0.794**	1.816***	6.386	−12.017**
	(0.411)	(1.046)	(0.313)	(0.323)	(13.918)	(4.329)
Observations	292	114	266	84	104	20
R^2	0.359	0.551	0.272	0.463	0.625	0.688
Adjusted R^2	0.345	0.526	0.255	0.421	0.602	0.651
Residual std. error	2.534 (df = 285)	3.061 (df = 107)	1.461 (df = 259)	0.625 (df = 77)	4.874 (df = 97)	4.852 (df = 17)
F statistic	26.592*** (df = 6; 285)	21.909*** (df = 6; 107)	16.139*** (df = 6; 259)	11.062*** (df = 6; 77)	26.928*** (df = 6; 97)	18.741*** (df = 2; 17)

Note: $^{*}p < 0.1$; $^{**}p < 0.05$; $^{***}p < 0.01$.

The effect of $log(ExposureDosis)$ was significant and negative (decreasing CVV) for all measurements, which was the case also for the previous models with/out interactions. The strongest effect was observed for ZnO (-3.067) and Cu (-3.136), while the weakest effect was noted for CeO_2 (-0.122) and SiO_2 (-0.289), which was primarily due to elemental characteristics. Regarding $ParticleDiameter$, there were contradictive results that varied across compounds. Only for three compounds, particle diameter was statistically significant; SiO_2 and Cu showed a positive relationship with particle size, while CeO_2 exhibited a negative effect. Positive effect indicated - the larger particles, the higher cell viability, the lower toxicity.

The results from these regressions indicate that HepaRG cells were particularly sensitive within most compounds (showing significant negative effects on viability) compared to the base A549 cells. Specifically, HepaRG cell lines were associated with a 2.418, 1.853, and 0.736 percentage point decrease in CVV for TiO_2, SiO_2, and CeO_2 (compared to A549 cell lines). This cell line was not significantly different from the base for ZnO, however, the HCT116 cell line was found to have a significantly negative effect on CVV (-5.764) in ZnO regression (compared to A549).

Interestingly, $ZnO\ NPs$ showed a positive and significant effect on HEPG2 and RAW267.7 cells, and $Ag\ NPs$ were positive and significant for all cell lines, with the highest positive effect of 5.796 for HEPG2. These results indicate that these cell lines might have had higher resistance to these NPs, or in the case of lower doses, $ZnO\ NPs$ or $Ag\ NPs$ could have acted as a nutrient, promoting cell growth or metabolic activity, which resulted in positive outcomes.

Multiple OLS model (cell viability by cell lines)

The aim was to explore how specific factors influence CVV separately for each cell line and whether these effects are consistent with the whole-sample results The base ($Constant$) for compounds were $Ag\ NPs$, which were selected to compare the effect of other compounds on cell viability, and the regression results are displayed in **Table 6** below.

Table 6. Results of multiple OLS model by cell lines.

	Dependent variable:				
	Viable cell count				
	A549	HCT116	HepaRG	HEPG2	RAW264.7
	(1)	(2)	(3)	(4)	(5)
log(ExposureDosis)	−0.615***	−0.917***	−1.203***	−0.712***	−0.722***
	(0.118)	(0.148)	(0.105)	(0.087)	(0.102)
ParticleDiameter	−0.004	−0.001	0.014	−0.009	−0.016
	(0.013)	(0.017)	(0.009)	(0.010)	(0.011)
CompoundsCeO_2	5.556***	3.252***	4.136 ***	0.979*	2.231***
	(0.738)	(0.922)	(1.102)	(0.534)	(0.626)
CompoundsCu	N/A	N/A	−6.033***	N/A	N/A
	N/A	N/A	(1.110)	N/A	N/A
CompoundsSiO_2	5.905***	3.351***	3.207***	0.559	1.831***
	(0.669)	(0.836)	(0.691)	(0.484)	(0.567)
CompoundsTiO_2	5.632***	3.022***	1.915**	0.561	2.394***
	(0.598)	(0.748)	(0.726)	(0.433)	(0.508)
CompoundsZnO	4.091**	−4.183*	−4.162***	1.375	2.540
	(1.820)	(2.276)	(1.432)	(1.317)	(1.545)
Constant	−4.420***	−2.039***	−2.216***	0.591	−0.817
	(0.601)	(0.751)	(0.683)	(0.470)	(0.551)
Observations	120	120	400	120	120
R^2	0.544	0.584	0.427	0.390	0.421
Adjusted R^2	0.519	0.562	0.417	0.357	0.390
Residual std. error	2.072 (df = 113)	2.590 (df = 113)	4.164 (df = 392)	1.499 (df = 113)	1.758 (df = 113)
F statistic	22.424*** (df = 6; 113)	26.488*** (df = 6; 113)	41.701 *** (df = 7; 392)	12.022*** (df = 6; 113)	13.673*** (df = 6; 113)

Note: $^{*}p < 0.1$; $^{**}p < 0.05$; $^{***}p < 0.01$.

Based on the results above, it is possible to see that the effect of $log(ExposureDosis)$ is statistically significant and negative for all observations, indicates universal trend of lower CVV while increasing exposure dose. The strongest negative effect was observed for HepaRG cells (-1.203), while the weakest negative effect was displayed for A549 (-0.615), emphasizing unique sensitivities of cell lines for specific exposure doses. Particle diameter was not found to be significantly associated to CVV in any of the cell line regressions.

The significant positive coefficients for CeO_2, SiO_2, and TiO_2 indicate lower toxicity in comparison to Ag across various cell lines (A549, HCT116, HepaRG and RAW264.7).

The effect of ZnO on CVV, compared to Ag, was significantly different in A549, HCT116 and HEPARG regressions. For A549 cell line, the effect of $ZnO\ NPs$ was positive (4.091), and for HCT116 (-4.183) and HepaRG (-4.162), the effect was negative. One of possible explanation could be that when interacting with A549, $ZnO\ NPs$ could promote cellular mechanisms to maintain viability, or for HCT116 and HepaRG could induce cytotoxic effects more strongly, leading to lower CVV.

The last negative instance was observed for $Cu\ NPs$ that were measured on HepaRG cell line, negatively affecting CVV by 6.033 percentage points. These results can be linked to either elemental

characteristics or HepaRG liver cells being particularly vulnerable due to their high metabolic activity and susceptibility to oxidative damage and metal ion toxicity.

Multiple OLS model (cell membrane damage by compound)

The aim was to explore how specific factors influence CMD separately for each compound. The base ($Constant$) for cell lines was HepaRG cell line, which was selected to compare the effect of other cell lines on CMD, and the regression results are displayed in **Table 7** below.

For $log(ExposureDosis)$, the effect is strong, significant and positive for all compounds, and especially strong for ZnO (17.93) and Ag (14.54), indicating they are highly toxic to membranes. Weaker effect was observed for Cu and CeO_2, but still statistically significant.

$ParticleDiameter$ is mostly non-significant, except TiO_2, where the damage to cell membranes is statistically significant, indicating that larger particles are less damaging. Nevertheless, there is no clear evidence on size-dependent pattern, suggesting that toxicity is driven more by chemical composition rather than size.

Regarding the effect of compounds, RAW264.7 displayed significantly higher sensitivity to Ag (109.1), SiO_2 (10.20), ZnO (25.51), possibly due to phagocytic cells being more vulnerable to membrane disruption by reactive or ion-releasing particles. For HEPG2, there is no significant response, based on the data, displaying possible resistance of cell line.

Multiple OLS model (cell membrane damage by cell line)

The aim was to explore how specific factors influence CMD separately for each cell line. The base ($Constant$) for compounds were $Ag\ NPs$, which were selected to compare the effect of other compounds on CMD, and the regression results are displayed in **Table 8** below.

The effect of $log(ExposureDosis)$ is strong, significant and positive for all three cell lines, where RAW264.7 shows the highest dose sensitivity (18.3), followed by HEPG2 (11.9) and HepaRG (3.2) indicating clear dose-response pattern.

$ParticleDiameter$ is significant only for HepaRG (-0.057), indicating that larger particles lead to less membrane damage. For HEPG2 and RAW264.7 the effect is not significant, demonstrating that particle size is not a consistent predictor across cell lines.

The effect of compounds compared to Ag is displaying wide range of results. The results for CeO_2, SiO_2 and TiO_2 are displaying similar significant negative effect on membrane damage for HEPG2 and RAW264.7 cell lines, while for HepaRG the effect is not significant, suggesting their relative safety compared to Ag or ZnO. When it comes to ZnO, the effect is significant and positive to HepaRG, indicating higher CMD, but for other two cell lines, it is non-significant.

Table 7. Results of multiple OLS model on CMD by compounds.

	Dependent variable:					
	Cell membrane damage					
	TiO_2	Ag	SiO_2	CeO_2	ZnO	Cu
	(1)	(2)	(3)	(4)	(5)	(6)
log(ExposureDosis)	5.540***	14.543**	2.513***	0.587***	17.930***	5.046**
	(0.630)	(5.616)	(0.583)	(0.179)	(2.610)	(1.801)
ParticleDiameter	−0.105*	−0.272	−0.030	0.071	1.130	−1.270
	(0.055)	(1.044)	(0.042)	(0.048)	(0.947)	(1.190)
ExposedCellHEPG2	4.537	27.640	5.004	−0.481	10.367	
	(2.752)	(27.322)	(3.696)	(0.754)	(11.889)	
ExposedCellRAW264.7	−2.391	109.105***	10.196***	−0.653	25.511**	
	(2.752)	(27.322)	(3.696)	(0.754)	(11.889)	
Constant	−3.855	−24.472	−2.348	−2.061	−188.568	6.041
	(2.412)	(32.225)	(2.602)	(1.434)	(137.655)	(14.243)
Observations	186	82	218	52	72	20
R^2	0.322	0.236	0.123	0.227	0.443	0.346
Adjusted R^2	0.307	0.196	0.106	0.161	0.410	0.269
Residual std. error	15.343 (df = 181)	93.370 (df = 77)	16.372 (df = 213)	2.249 (df = 47)	40.192 (df = 67)	15.964 (df = 17)
F statistic	21.497*** (df = 4; 181)	5.935*** (df = 4; 77)	7.463*** (df = 4; 213)	3.445** (df = 4; 47)	13.322*** (df = 4; 67)	4.496** (df = 2; 17)

Note: $^{*}p < 0.1$; $^{**}p < 0.05$; $^{***}p < 0.01$.

Table 8. Results of multiple OLS model on CMD by cell lines.

	Dependent variable:		
	Cell membrane damage		
	HepaRG	HEPG2	RAW264.7
	(1)	(2)	(3)
log(ExposureDosis)	3.246***	11.887***	18.319***
	(0.314)	(1.951)	(4.550)
ParticleDiameter	−0.057**	−0.077	0.004
	(0.028)	(0.217)	(0.507)
CompoundsCeO2	−2.461	−31.505***	−113.673***
	(3.254)	(12.025)	(28.047)
CompoundsCu	−0.339		
	(3.277)		
CompoundsSiO2	−0.310	−24.635**	−100.909***
	(2.041)	(10.901)	(25.426)
CompoundsTiO2	3.467	−20.868**	−109.397***
	(2.180)	(9.757)	(22.758)
CompoundsZnO	21.535***	5.685	−70.821
	(4.235)	(29.680)	(69.228)
Constant	−2.618	5.674	70.022***
	(2.020)	(10.595)	(24.713)
Observations	390	120	120
R^2	0.311	0.301	0.275
Adjusted R^2	0.298	0.264	0.236
Residual std. error	12.300 (df = 382)	33.776 (df = 113)	78.780 (df = 113)
F statistic	24.604*** (df = 7; 382)	8.104*** (df = 6; 113)	7.143*** (df = 6; 113)

Note: $^{*}p < 0.1$; $^{**}p < 0.05$; $^{***}p < 0.01$.

Multiple OLS model (mitochondrial membrane potential by compound)

The aim was to explore how specific factors influence MMP separately for each compound. The base ($Constant$) for cell lines was HepaRG cell line, which was selected to compare the effect of other cell lines on MMP, and the regression results are displayed in **Table 9** below.

For $log(ExposureDosis)$, the effect is significant for all compounds except SiO_2, but effects are varying. For TiO_2, Ag, ZnO and Cu - the effect is negative. For ZnO (-1.70) and Cu (-1.29) the effect is showing strongest depolarizing effects. CeO_2 shows a positive effect (0.29), indicating preservation or enhancement of MMP - consistent with antioxidant properties.

Table 9. Results of multiple OLS model on MMP by compounds.

	Dependent variable:					
	Mitochondrial membrane potential					
	TiO2	Ag	SiO2	CeO2	ZnO	Cu
	(1)	(2)	(3)	(4)	(5)	(6)
log(ExposureDosis)	−0.325***	−1.041***	0.015	0.292***	−1.703***	−1.287***
	(0.066)	(0.236)	(0.036)	(0.087)	(0.213)	(0.196)
ParticleDiameter	0.013**	−0.082*	−0.005*	0.001	0.118	0.378***
	(0.006)	(0.044)	(0.003)	(0.023)	(0.077)	(0.130)
ExposedCellHEPG2	−0.088	−1.784	−0.686***	−1.058***	1.092	
	(0.287)	(1.148)	(0.231)	(0.366)	(0.970)	
ExposedCellRAW264.7	0.450	−3.347***	0.033	−0.703*	0.487	
	(0.287)	(1.148)	(0.231)	(0.366)	(0.970)	
Constant	−0.363	4.129***	−0.396**	−0.179	−15.509	−8.939***
	(0.252)	(1.354)	(0.163)	(0.696)	(11.233)	(1.554)
Observations	186	82	218	52	72	20
R^2	0.156	0.281	0.050	0.301	0.502	0.752
Adjusted R^2	0.137	0.244	0.032	0.242	0.472	0.722
Residual std. error	1.601 (df = 181)	3.924 (df = 77)	1.024 (df = 213)	1.092 (df = 47)	3.280 (df = 67)	1.741 (df = 17)
F statistic	8.334*** (df = 4; 181)	7.526*** (df = 4; 77)	2.812** (df = 4; 213)	5.060*** (df = 4; 47)	16.895*** (df = 4; 67)	25.712*** (df = 2; 17)

Note: $^{*}p < 0.1$; $^{**}p < 0.05$; $^{***}p < 0.01$.

$ParticleDiameter$ is displaying significant effects, whereas for TiO_2 and Cu it indicates that larger particles are associated with increased MMP, possibly indicating less bioactive/toxic behavior with size, and for Ag and SiO_2 the effect is opposite, displaying that smaller particles are more damaging.

Regarding the effect of compounds compared to HepaRG, the effect of HEPG2 is significantly more sensitive (lower MMP) for SiO_2 (-0.69) and CeO_2 (-1.06), and RAW264.7 is highly sensitive to Ag (-3.35), indicating macrophage vulnerability.

Multiple OLS model (mitochondrial membrane potential by cell line)

The aim was to explore how specific factors influence MMP separately for each cell line. The base ($Constant$) for compounds were $Ag\ NPs$, which were selected to compare the effect of other compounds on MMP, and the regression results are displayed in **Table 10** below.

The effect of $log(ExposureDosis)$ is strong, significant and negative for all three cell lines, where RAW264.7 shows the highest dose sensitivity (-0.585), followed by HEPG2 (-0.532) and HepaRG (-0.387) indicating clear dose-response pattern.

$ParticleDiameter$ is not significant for any cell line, suggesting that size alone does not systematically impact mitochondrial toxicity when controlling for compound and dose.

For the effect of compounds, CeO_2, the effect is positive for all three cell lines, but statistically significant only for HEPG2 and RAW264.7. Next, CeO_2 is the only compound with consistently positive effects on MMP, reinforcing its protective/antioxidant profile. For Cu, data are available only for HepaRG cells, where the effect is negative and significant (-7.482), displaying that Cu might be severely toxic to liver-like cells. For both SiO_2 and TiO_2 the effect is similar, having statistically significant positive effect on RAW264.7 cells, possibly due to cell immune mechanisms.

Table 10. Results of multiple OLS model on MMP by cell lines.

	Dependent variable:		
	Mitochondrial membrane potential		
	HepaRG	HEPG2	RAW264.7
	(1)	(2)	(3)
log(ExposureDosis)	−0.387***	−0.532***	−0.585***
	(0.062)	(0.119)	(0.157)
ParticleDiameter	−0.001	−0.011	0.017
	(0.006)	(0.013)	(0.017)
CompoundsCeO2	0.979	1.361*	3.098***
	(0.646)	(0.732)	(0.968)
CompoundsCu	−7.482***		
	(0.650)		
CompoundsSiO2	−0.124	0.652	2.934***
	(0.405)	(0.664)	(0.877)
CompoundsTiO2	−0.512	0.860	2.914***
	(0.433)	(0.594)	(0.785)
CompoundsZnO	−1.890**	1.725	−0.812
	(0.840)	(1.807)	(2.389)
Constant	0.546	−0.304	−2.299***
	(0.401)	(0.645)	(0.853)
Observations	390	120	120
R^2	0.373	0.178	0.231
Adjusted R^2	0.361	0.134	0.190
Residual std. error	2.441 (df = 382)	2.057 (df = 113)	2.719 (df = 113)
F statistic	32.457*** (df = 7; 382)	4.071*** (df = 6; 113)	5.651*** (df = 6; 113)

Note: $^{*}p < 0.1$; $^{**}p < 0.05$; $^{***}p < 0.01$.

Multiple OLS model (nuclear intensity by compound)

The aim was to explore how specific factors influence Nuclear Intensity separately for each compound. The base ($Constant$) for cell lines was HepaRG cell line, which was selected to compare the effect of other cell lines on Nuclear Intensity, and the regression results are displayed in **Table 11** below.

For $log(ExposureDosis)$, the effect is mostly positive and significant. ZnO shows the strongest effect (2.512), followed by Ag (1.107) and TiO_2 (1.021), while Cu shows a non-significant negative coefficient, suggesting it may behave differently or that data is limited ($n = 20$). Overall, results indicate that nuclear intensity increases with dosage.

$ParticleDiameter$ is displaying generally non-significant effects, except TiO_2 (0.020) and CeO_2 (0.039), where mild positive effects is displayed. For $Cu\ NPs$, results show a strong positive effect (0.698), suggesting that larger Cu particles may increase nuclear intensity.

The effect on cell lines is visible primarily for $Ag\ NPs$, where results show significantly higher nuclear intensity compared to HepaRG. For SiO_2 on RAW264.7, results also show significantly higher nuclear intensity, but for TiO_2, CeO_2, or ZnO, there are no significant cell line effects. This suggests that Ag

and SiO_2 may cause stronger nuclear intensity increases specifically in immune or liver cells (RAW264.7 and HEPG2).

Multiple OLS model (nuclear intensity by cell line)

The aim was to explore how specific factors influence Nuclear Intensity separately for each cell line. The base ($Constant$) for compounds were $Ag\ NPs$, which were selected to compare the effect of other compounds on Nuclear Intensity, and the regression results are displayed in **Table 12** below.

The effect of $log(ExposureDosis)$ is strong, significant and positive for all three cell lines, suggesting a dose-dependent increase in nuclear intensity, likely linked to cellular stress, chromatin changes, or genotoxic responses. For RAW264.7 (macrophages), results show the steepest response (1.97), indicating high sensitivity.

$ParticleDiameter$ is displaying mostly non-significant effect except for RAW264.7, where larger particles increase nuclear intensity (0.060), possibly reflecting particle uptake or size-dependent stress response in phagocytic cells.

For HepaRG cell line, ZnO stands out with a large positive effect (3.99), compared to other cell types, and Cu causes a strong reduction (-3.59), indicating a highly toxic effect. Other compounds are mostly not significant, suggesting HepaRG may be more resilient or exhibit a different stress pattern. The results for HEPG2 and RAW264.7 are displaying strong negative effects from more compounds: CeO_2, SiO_2, TiO_2 and ZnO, suggesting that these compounds reduce nuclear intensity, possibly indicating nuclear damage, or toxicity leading to nuclear fading.

Table 11. Results of multiple OLS model on nuclear intensity by compounds.

	Dependent variable:					
	Nuclear Intensity					
	TiO2	Ag	SiO2	CeO2	ZnO	Cu
	(1)	(2)	(3)	(4)	(5)	(6)
log(ExposureDosis)	1.021***	1.107***	0.637***	0.586***	2.512***	−0.285
	(0.120)	(0.338)	(0.065)	(0.074)	(0.314)	(0.506)
ParticleDiameter	0.020*	0.024	−0.004	0.039*	0.003	0.698*
	(0.010)	(0.063)	(0.005)	(0.020)	(0.114)	(0.334)
ExposedCellHEPG2	−0.640	4.339**	0.500	0.078	−2.071	
	(0.526)	(1.646)	(0.414)	(0.311)	(1.432)	
ExposedCellRAW264.7	0.654	4.077**	1.113***	0.222	−0.984	
	(0.526)	(1.646)	(0.414)	(0.311)	(1.432)	
Constant	−1.552***	−2.396	−1.047***	−1.651***	−1.890	−9.695**
	(0.461)	(1.941)	(0.291)	(0.591)	(16.578)	(4.003)
Observations	186	82	218	52	72	20
R^2	0.307	0.216	0.332	0.590	0.496	0.216
Adjusted R^2	0.292	0.175	0.319	0.555	0.466	0.124
Residual std. error	2.934 (df = 181)	5.625 (df = 77)	1.834 (df = 213)	0.928 (df = 47)	4.840 (df = 67)	4.487 (df = 17)
F statistic	20.067*** (df = 4; 181)	5.295*** (df = 4; 77)	26.437*** (df = 4; 213)	16.919*** (df = 4; 47)	16.514*** (df = 4; 67)	2.340 (df = 2; 17)

Note: $^{*}p < 0.1$; $^{**}p < 0.05$; $^{***}p < 0.01$.

Table 12. Results of multiple OLS model on MMP by cell lines.

	Dependent variable:		
	Nuclear intensity		
	HepaRG	HEPG2	RAW264.7
	(1)	(2)	(3)
log(ExposureDosis)	0.732***	1.230***	1.968***
	(0.072)	(0.184)	(0.293)
ParticleDiameter	−0.002	0.015	0.060*
	(0.006)	(0.021)	(0.033)
CompoundsCeO2	−0.052	−4.297***	−4.183**
	(0.746)	(1.136)	(1.807)
CompoundsCu	−3.590***		
	(0.751)		
CompoundsSiO2	−0.491	−4.166***	−3.292**
	(0.468)	(1.030)	(1.638)
CompoundsTiO2	0.378	−4.407***	−2.926**
	(0.500)	(0.922)	(1.466)
CompoundsZnO	3.990***	−4.480	−8.736*
	(0.971)	(2.803)	(4.459)
Constant	−0.850*	1.812*	−1.124
	(0.463)	(1.001)	(1.592)
Observations	390	120	120
R^2	0.358	0.387	0.328
Adjusted R^2	0.346	0.354	0.293
Residual std. error	2.820 (df = 382)	3.190 (df = 113)	5.074 (df = 113)
F statistic	30.420*** (df = 7; 382)	11.871*** (df = 6; 113)	9.202*** (df = 6; 113)

Note: $^{*}p < 0.1$; $^{**}p < 0.05$; $^{***}p < 0.01$.

Multiple OLS model (nuclear size by compound)

The aim was to explore how specific factors influence Nuclear Size separately for each compound. The base ($Constant$) for cell lines was HepaRG cell line, which was selected to compare the effect of other cell lines on Nuclear Size, and the regression results are displayed in **Table 13** below.

For $log(ExposureDosis)$, the effect is significant for most of compounds, except Ag and SiO_2. Exposure dose increases nuclear size for TiO_2, CeO_2, and ZnO, but decreases it for Cu - indicating compound-specific effects.

The effect of $ParticleDiameter$ displays significant positive effect on nuclear size for TiO_2 (0.015), ZnO (0.301), and Cu (1.921), suggesting particle size matters for some, but not all, materials. It also indicates that larger particles are causing less nuclear shrinkage, supporting that larger particles are less toxic.

Regarding the effect of compounds compared to HepaRG is visible as for HEPG2, all results are significant and having negative effect on nuclear size, while for RAW264.7, the results are very similar except SiO_2 where results are non-significant. These results indicate that cell type matters, as HepG2 and RAW264.7 show nuclear shrinkage, highlighting cell-specific sensitivity to NP exposure.

Table 13. Results of multiple OLS model on MMP by compounds.

	Dependent variable:					
	Nuclear size					
	TiO_2	Ag	SiO_2	CeO_2	ZnO	Cu
	(1)	(2)	(3)	(4)	(5)	(6)
log(ExposureDosis)	0.171***	0.396	−0.034	0.158***	1.442***	−4.041***
	(0.060)	(0.266)	(0.044)	(0.048)	(0.436)	(1.151)
ParticleDiameter	0.015***	0.048	−0.001	0.010	0.301*	1.921**
	(0.005)	(0.049)	(0.003)	(0.013)	(0.158)	(0.761)
ExposedCellHEPG2	−1.676***	−5.922***	−1.403***	−1.433***	−5.762***	
	(0.260)	(1.294)	(0.278)	(0.203)	(1.988)	
ExposedCellRAW264.7	−0.446*	−6.388***	−0.133	−0.801***	−5.363***	
	(0.260)	(1.294)	(0.278)	(0.203)	(1.988)	
Constant	0.187	1.430	0.528***	0.267	−42.889*	−12.658
	(0.228)	(1.527)	(0.196)	(0.386)	(23.014)	(9.108)
Observations	186	82	218	52	72	20
R^2	0.236	0.364	0.113	0.569	0.285	0.524
Adjusted R^2	0.219	0.331	0.096	0.532	0.243	0.468
Residual std. error	1.450 (df = 181)	4.423 (df = 77)	1.232 (df = 213)	0.606 (df = 47)	6.720 (df = 67)	10.209 (df = 17)
F statistic	13.967*** (df = 4; 181)	11.007*** (df = 4; 77)	6.792*** (df = 4; 213)	15.483*** (df = 4; 47)	6.685*** (df = 4; 67)	9.345*** (df = 2; 17)

Note: $^{*}p < 0.1$; $^{**}p < 0.05$; $^{***}p < 0.0$.

Multiple OLS model (nuclear size by cell line)

The aim was to explore how specific factors influence Nuclear Size separately for each cell line. The base ($Constant$) for compounds were $Ag\ NPs$, which were selected to compare the effect of other compounds on Nuclear Size, and the regression results are displayed in **Table 14** below.

The effect of $log(ExposureDosis)$ is significant for HepaRG (0.248) and for HEPG2 (-0.575), while for RAW264.7 it is non-significant. This contrast across all three cell lines displays cell-specific response.

Table 14. Results of multiple OLS model on MMP by cell lines.

	Dependent variable:		
	Nuclear size		
	HepaRG	HEPG2	RAW264.7
	(1)	(2)	(3)
log(ExposureDosis)	0.248**	−0.575***	0.085
	(0.120)	(0.115)	(0.133)
ParticleDiameter	0.007	0.004	0.039**
	(0.011)	(0.013)	(0.015)
CompoundsCeO2	−2.674**	2.038***	2.913***
	(1.244)	(0.709)	(0.817)
CompoundsCu	−4.758***		
	(1.253)		
CompoundsSiO2	−3.297***	1.602**	3.338***
	(0.780)	(0.643)	(0.741)
CompoundsTiO2	−2.673***	1.820***	3.459***
	(0.833)	(0.575)	(0.663)
CompoundsZnO	−0.198	0.470	−2.962
	(1.619)	(1.750)	(2.016)
Constant	2.821***	−1.278**	−4.020***
	(0.772)	(0.625)	(0.720)
Observations	390	120	120
R^2	0.104	0.251	0.262
Adjusted R^2	0.088	0.211	0.223
Residual std. error	4.702 (df = 382)	1.991 (df = 113)	2.294 (df = 113)
F statistic	6.337*** (df = 7; 382)	6.304*** (df = 6; 113)	6.698*** (df = 6; 113)

Note: $^{**}p < 0.05$; $^{***}p < 0.01$.

$ParticleDiameter$ is significant only for RAW264.7, where the effect is positive (0.039), indicating that larger particles lead to nuclear enlargement, or, that nucleus size is less damaged compared to smaller particles.

The effect of other compounds on HepaRG is displaying sensitiveness to Cu (-4.758), SiO_2 (-3.297), TiO_2 (-2.673), with dose-related enlargement. HEPG2 cells react oppositely to HepaRG—they shrink with increasing dose but increase nuclear size in response to CeO_2 (2.038), SiO_2 (1.602), and TiO_2 (1.820). This suggests compound-specific hypertrophy and dose-driven cytotoxicity. RAW264.7 cells show nuclear enlargement driven primarily by particle diameter and compound type, especially CeO_2 (2.913), SiO_2 (3.338), and TiO_2 (3.459). Dose has no significant effect, indicating size and chemistry dominate the nuclear response.

Discussion

The results above represent an exemplary attempt at a comprehensive statistical analysis of the data extracted from the NanoCommons database. Among a large number of available datasets, the attention is focused on six widely studied compounds in the form of NPs and their concentration effects on different cell lines while their size is also considered as the factor. The compounds selected from the database were zinc oxide (ZnO), copper (Cu), silver (Ag), titanium dioxide (TiO_2), silicon dioxide (SiO_2), and cerium dioxide (CeO_2), where each compound exhibited distinct toxicological behaviors associated with its properties, such as ion release, oxidative stress induction, or photocatalytic activity. The logical counterpart in consideration of any toxic agent effects is the living target, represented in vitro by the various cell lines derived from different tissues having thus different susceptibility and response to the questioned toxic agent. The toxicity effect was evaluated on HepG2, HepaRG, A549, RAW264.7, and HCT116 cell lines, while the following markers were in the scope: Cell membrane damage which reflects the physical integrity of the plasma membrane, Mitochondrial membrane potential ($\Delta\Psi m$) representing mitochondrial health and energy production, Nuclear intensity and Nuclear size to capture the response of nucleus, and finally, Cell Viability as the last endpoint, quantifying the proportion of live versus dead cells.

Limitation of study

Prior to any other consideration, it should also be acknowledged that this study has several limitations. First, the analysis was conducted on the limited dataset, although being extracted from the dataset is as representative as possible. Moreover, factors such as shape, surface charge or modifications of NPs were not included in this study as they were not included in the original database and present the challenge for the future research. Once there is sufficient amount of data on the other key parameters, it would be possible to perform aggregated analysis and evaluate the impact of the named parameters. Next, the analysis is done in full awareness that the statistic evaluation enables us to find correlations without establishing causality relations.

Analysis of trends - cell viability

The results of statistical analysis of different variables affecting CVV displayed wide range of findings in terms of interactions of various compounds, cell lines and NPs size. Their graphical visualization in the form of the interactive $3D$ chart as well as their statistics are available in **supplementary data** of

the paper. In all models, the exposure dose was consistently displaying significant negative effect on CVV, which is supporting the universal trend of increased toxicity at higher doses, as can be seen in **Figure 2**.

Another principal view on the data shown in **Figure 3** demonstrates the analysis of trends in CVV dependence on particle diameter.

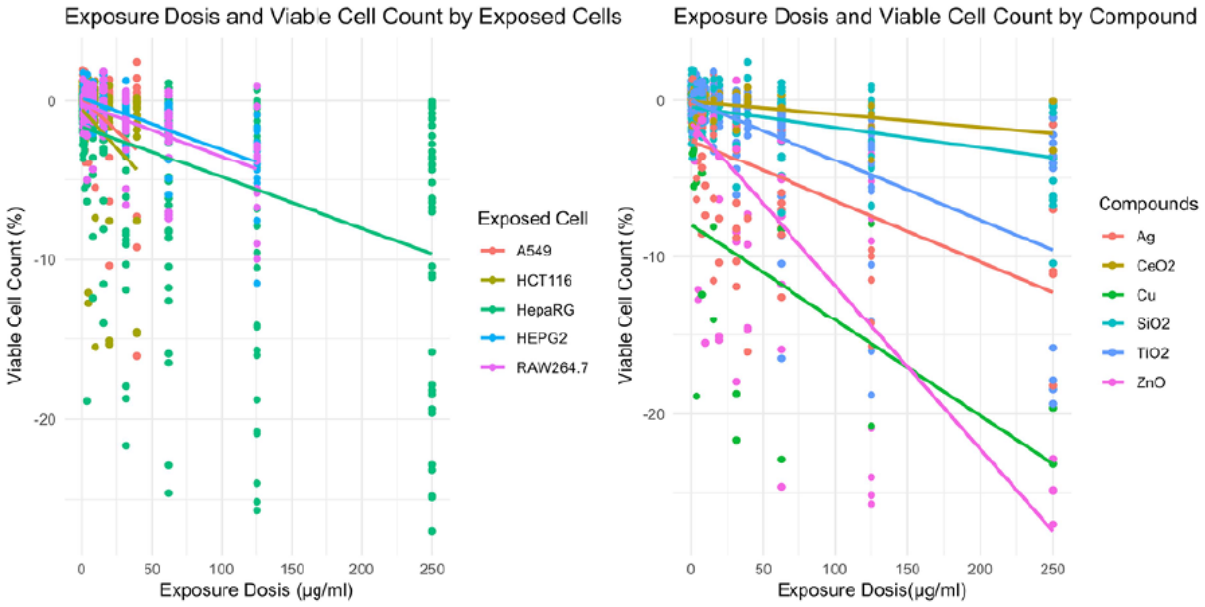


Figure 2. Effect of $ExposureDosis$ on CVV from perspective of exposed cells (left) and compounds (right). Note that the $2D$ projection of an originally $3D$ graph may lead to distortions in the apparent lengths of displayed line segments

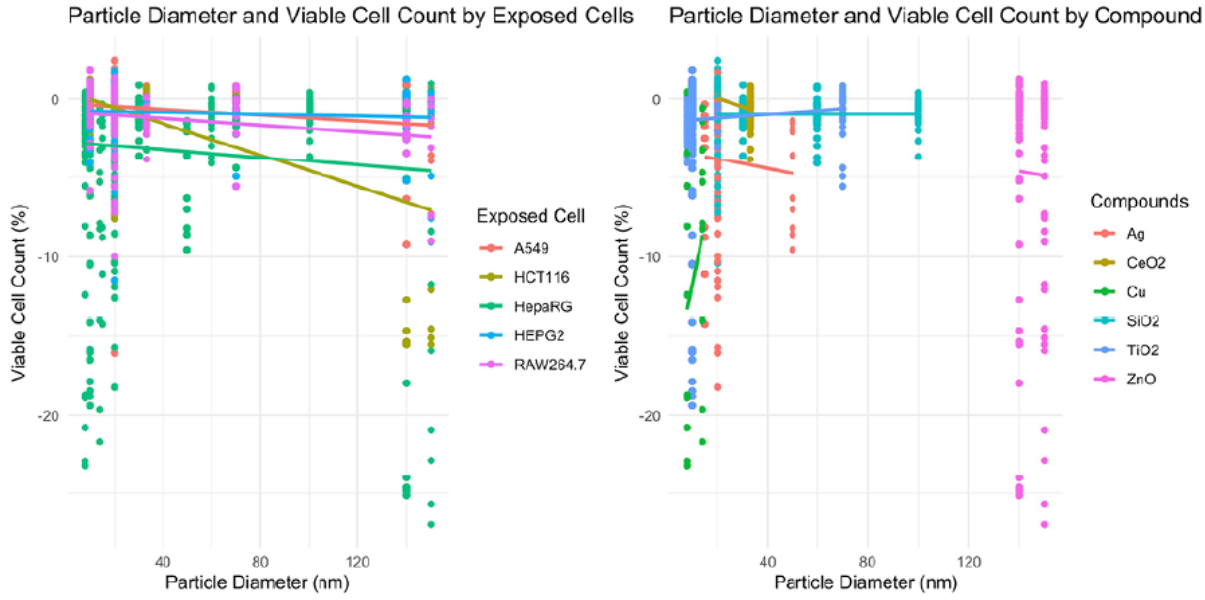


Figure 3. Effect of $ParticleDiameter$ on CVV from perspective of exposed cells (left) and compounds (right). Note that the $2D$ projection of an originally $3D$ graph may lead to distortions in the apparent lengths of displayed line segments

The particle size, although displaying negligible overall effect on CVV, showed compounds-specific impact in the model with interactions, particularly for $Cu\ NPs$ where the increase in particle size was associated with positive effect on CVV (0.776), thus decreasing the total negative effect of $Cu\ NPs$ on

CVV. The results from model without interactions displayed that Cu and ZnO were associated with negative impact on CVV as expected (**Ahamed et al. 2010; Fahmy and Cormier 2009; Fukui et al. 2012; Naz, Gul, and Zia 2020; Song et al. 2010**) while CeO_2, SiO_2 and TiO_2 were displaying positive effect on CVV, due to each compound characteristics - CeO_2 possibly behaving as a prooxidant (**Pansambal et al. 2023; Singh et al. 2020**), and TiO_2 possibly behaving relatively inert unless photo-activated (**Arun et al. 2023; Baranowska-Wójcik et al. 2020; Ziental et al. 2020**). In the case of SiO_2 there is no clear explanation why SiO_2 nanoparticles resulted to have positive effect on CVV. There are numerous studies displaying contradictory conclusions of SiO_2 toxicity, primarily focusing on the factor of surface modification (**Marzaioli et al. 2014; Nayl et al. 2022; Yang et al. 2018**), which in this study, had not been examined.

Results from OLS models for toxicity markers

The results from OLS model for toxicity markers is possible to display in the compiled form, which is shown in **Table 15**. The table provides unique view which enables to see similarities or differences across predictors and their level of significance. To enable data aggregation, the significance levels obtained for individual correlations needed to be evaluated collectively. For each predictor, both the average significance score and the maximum significance score were calculated. If the difference between the maximum and the average score exceeded 2, the predictor was considered non-significant overall. Conversely, if the difference was 2 or less (i.e., 0 or 1), the average score was used as the final significance level.

Table 15. Compiled results from OLS models.

Predictor	Cell Membrane Damage (CMD)	Mitochondrial Membrane Potential (MMP)	Nuclear Intensity (NI)	Nuclear Size (NS)	Viable Cell Count (VCC)
Dose (log scale)	↑ ***	↓ ***	↑ ***	↑ ↓**	↓ ***
Particle Diameter	↑ ↓ (non-sig)	↑ ↓ (non-sig)	↑ (non-sig)	↑ (non-sig)	↑ ↓ (non-sig)
Compound: Ag	↑ (non-sig)	↓ (non-sig)	↑ ↓*	↓ ***	↓ **
Compound: ZnO	↑ (non-sig)	↓ (non-sig)	↑ ↓ (non-sig)	↓ (non-sig)	↓ (non-sig)
Compound: Cu	↓ (non-sig)	↓ ***	↓ ***	↓ ***	↓ ***
Compound: CeO_2	↓ **	↑ (non-sig)	↓ **	↑ ***	↑ ***
Compound: SiO_2	↓ ***	↑ (non-sig)	↓ **	↑ ***	↑ ***
Compound: TiO_2	↓ ***	↑ (non-sig)	↓ **	↑ ***	↑ ***
Cell Line: HepaRG	↓ (non-sig)	↓ (non-sig)	↓ **	↑ (non-sig)	↓ **
Cell Line: HCT116	No data	No data	No data	No data	↓ (non-sig)
Cell Line: HEPG2	↑ (non-sig)	↓ (non-sig)	↑ (non-sig)	↓ ***	↑ ↓**
Cell Line: RAW264.7	↑ **	↓ (non-sig)	↑ (non-sig)	↓ ***	↑ ↓**
Cell Line: A549	No data	No data	No data	No data	↑ **

Legend:.↓: Negative effect on toxicity marker ↑: Positive effect on toxicity marker ↑ ↓: No clear direction of effect on toxicity marker No data: no data for measurement non-sig//**/***: Overall significance score*

Based on the results above, we can see that for some variables, the mechanistic interrelationship between toxicity markers, according to the **Figure 1** is confirmed, while for some there was not enough evidence and mixed pathway was indicated. When it comes to dose (log scale), it is the single strongest driver of toxicity across all predictors, as every endpoint changes significantly with increased dose. On the other hand, nanoparticle size is not a strong predictor, as within the studied range, it did not reach significance and displayed only not-significant results. Next, focusing on NI and NS, different stages of cell damage can be observed:

- $\uparrow NI$ & $\downarrow NS$ = chromatin condensation → early apoptosis/stress
- $\downarrow NI$ & $\uparrow NS$ = nuclear swelling → necrosis/late apoptosis
- Both ↑ or both ↓ = mixed cell-cycle effects or late-stage debris

Among the tested compounds, the uniformly toxic is Cu, and the results support a mitochondria-driven apoptotic sequence (MMP loss $\rightarrow$ nuclear changes $\rightarrow \downarrow VCC$) with minimal early membrane involvement (CMD $\downarrow$ non sig). For CeO_2, SiO_2, TiO_2, compounds, these oxides display partial protective effects, as they reduce membrane damage ($\downarrow CMD$), increase nuclear size ($\uparrow NS$), and maintain higher viable cell counts ($\uparrow CVV$), although effect on mitochondria ($\uparrow MMP$) is not statistically significant and for that reason should be interpreted cautiously, as it indicates adaptive/low-toxicity behavior under these conditions rather than a canonical injury cascade.

For the remaining two compounds - both shows mixed signals, while for Au, the modest but significant reductions in nuclear integrity and viability is visible, while ZnO exhibits weak, non-significant trends toward toxicity.

HepaRG cells display moderate mitochondrial and nuclear impairment ($\downarrow MMP$, $\downarrow NI$), accompanied by reduced viability ($\downarrow CVV$), though effects are generally weaker compared to other lines. HEPG2 & RAW264.7 show increased membrane damage ($\uparrow CMD$) and nuclear shrinkage ($\downarrow NS$), but mixed viability, and A549 and HCT116 were only assayed for viability: both trend toward fewer live cells at higher treatment, though only A549 is significant. It can be concluded that for cell lines, macrophage-like RAW264.7 and hepatocyte-like HepG2 show pronounced membrane and nuclear damage, whereas HepaRG shows relatively less.

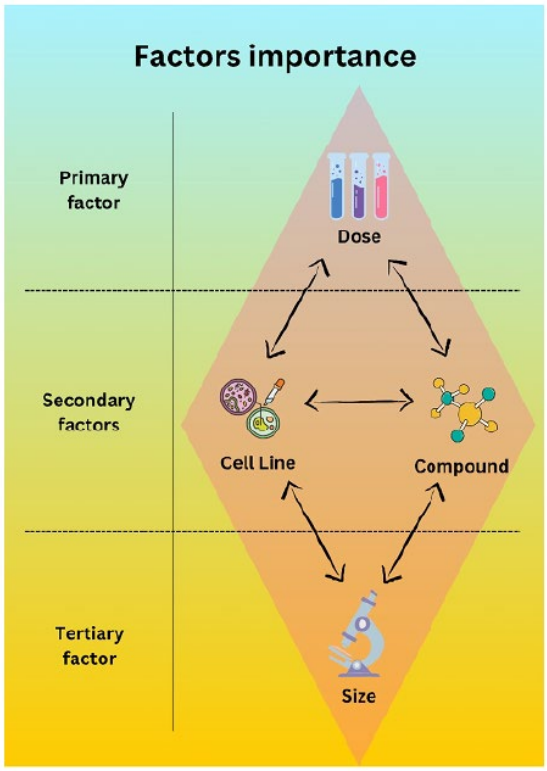


Figure 4. Factors importance in nanoparticles toxicity.

Hierarchy of investigated factors

The results have indicated a hierarchy within the four investigated factors influencing the toxicity scores of NPs on various toxicity markers, as illustrated in **Figure 4**. First, from the investigated predictors, dose emerges as the primary driver of toxicity, as it significantly affects all endpoints. Next

is compound and cell line, as they play major roles, especially in modulating mitochondrial and nuclear effects. On the last place is particle size, while mechanistically important, it did not reach statistical significance under the analyzed conditions. This conclusion is contra-intuitive when assuming the key role of size-related effects in nanomaterials, including the nanotoxicity as revealed by many experimental mechanistic studies (**Macko et al. 2022**) and references therein). It should be kept in mind that these results do not suggest that the size of NPs does not play any role in their toxicity mechanism (e.g. for Ag, TiO_2, and ZnO in this study), but the effect of various sizes has not been significantly manifested at testing conditions used in the original studies collected and integrated into the NanoCommons knowledge base.

Correlation to in vivo studies and AI models

A recent meta-study of in vivo measurements on similar topic examined 13 different nanomaterials from more than 100 peer reviewed articles to determine their $NOAEC$ No-Observed-Adverse-Effect Concentration) and $LOAEC$ (Lowest-Observed-Adverse-Effect Concentration). Among other findings, authors concluded positive correlation between particle size and $NOAEC/LOAEC$, most likely due to the larger particles requiring a higher concentration to observe an adverse effect compared to smaller particles (**Hadrup et al. 2023**).

Another study is investigating use of Artificial Intelligence (AI) and Machine Learning (ML) when assessing the toxicity of nanoparticles and nanomaterials. The article is stressing the importance of available sources and at the same time highlighting the challenges stemming from both statistical and biological point of view (**Singh et al. 2023**).

Both these articles are supporting the need for reliable and consistent data sources as well as standardized benchmarks to evaluate the still-emerging hazard related to nanoparticles toxicity.

Future research

When it comes to the future research of nanoparticles toxicity, and at the same time, enrichment of NanoCommons database, it would be beneficial to have more data on toxicity of Alumina NPs (Al_2O_3), which can release Al^{3+} ions, which are known to be neurotoxic and can interfere with cellular functions (**Gao et al. 2022; Park et al. 2016, 2015; Strigul et al. 2009**). To complete the picture of the most produced nanoparticles, Carbonaceous NPs should be subject to continuous research, as these also poses toxicological properties (**Awasthi et al. 2024; Uo et al. 2011**). Another addition to the database could be done on ultrafine dust particles ($UFPs$) collected at different locations. $UFPs$ consist of particles below 100 nanometers, and pose various risks (cancer, neurological or respiratory health issues), at the same time, it is the most common nanoparticle in the environment (**Hammond et al. 2022; Heinzerling, Hsu, and Yip 2016; Kolling et al. 2011; Ophir et al. 2019**). For the reasons above, addition and toxicological research on the abovementioned elements could enhance the relevance of the database and its metanalysis.

Conclusion

This study provides insights into the relationships between nanoparticle characteristics and cell viability. The effects of variables - NPs composition, cell line, dose and NPs size were explored via two main models - the first model was a Multiple OLS Model without interactions (Model 1), aimed at

exploring the significance of certain variables and their effect on cell viability without considering any interactions. The second was a Multiple OLS Model with interactions (Model 2), which aimed to explore the significance of certain variables on cell viability while also considering interactions between some of the regressors. Subsequently, sensitivity analyses were conducted by sub setting the final sample and extending the analysis to additional toxicity markers: Cell Membrane Damage, Mitochondrial Membrane Potential, Nuclear Intensity, and Nuclear Size.

First, the relationship between the independent variables and toxicity markers by compounds were explored. Second, the sample was divided based on cell lines. The results displayed significant dose dependency on all toxicity markers, across all models and confirmed the universal Paracelsian trend of increased toxicity at higher doses. The particle size had an almost negligible effect, but compound-specific impacts were observed. While particle size did not show significant influence, cell line-specific effects in all directions were observed - particularly for HepaRG, RAW264.7, and HEPG2 - though these effects were more variable and endpoint-specific compared to the consistent dose dependency.

The results of the analysis can be generalized by ordering the factors within a hierarchy of influence. The dose was determined as the primary factor, displaying consistent and significant effects across all toxicity markers. Next-highest important factors are compound and cell line, which influence specific markers such as mitochondrial potential, membrane damage, or nuclear changes. The particle size was manifested to be of lowest importance, as it did not reach significant effect on toxicity markers, under the studied conditions.

Moreover, this study also demonstrated the usefulness of data collections present in the NanoCommons database and indicates its future potential for data extraction in the field of nanotoxicity. The amount of gathered $FAIR$ (Findable, Accessible, Interoperate, and Reusable) data surpasses the magnitude of any individual experimental study. The observed correlations may be a stepping stone for targeting new studies and developing more sensitive nanotoxicity testing methods to help bridge the gap between mechanistic and statistical screening studies.

References

Abbasi, R., G. Shineh, M. Mobaraki, S. Doughty, and L. Tayebi. **2023**. "Structural Parameters of Nanoparticles Affecting Their Toxicity for Biomedical Applications: A Review" Journal of Nanoparticle Research 25 (3): 43. **https://doi.org/10.1007/s11051-023-05690-w**.

Ahamed, M., M. J. Akhtar, and H. A. Alhadlaq. **2020**. "Influence of Silica Nanoparticles on Cadmium-Induced Cytotoxicity, Oxidative Stress, and Apoptosis in Human Liver HepG2 Cells" Environmental Toxicology 35 (5): 599-608. **https://doi. org/10.1002/tox.22895**.

Ahamed, M., M. J. Akhtar, and H. A. Alhadlaq. **2019**. "Preventive Effect of TiO_2 Nanoparticles on Heavy Metal Pb-Induced Toxicity in Human Lung Epithelial (A549) Cells." Toxicology in Vitro 57: 18-27. **https://doi.org/10.1016/j.tiv.2019.02.004**.

Ahamed, M., M. A. Siddiqui, M. J. Akhtar, I. Ahmad, A. B. Pant, and H. A. Alhadlaq. **2010**. "Genotoxic Potential of Copper Oxide Nanoparticles in Human Lung Epithelial Cells." Biochemical and Biophysical Research Communications 396 (2): 578-583. **https://doi.org/10.1016/j.bbrc.2010.04.156**.

Ahmad, J., M. A. Siddiqui, M. J. Akhtar, H. A. Alhadlaq, A. Alshamsan, S. T. Khan, R. Wahab, et al. **2018**. "Copper Doping Enhanced the Oxidative Stress-Mediated Cytotoxicity of TiO_2 Nanoparticles in A549

Cells" Human & Experimental Toxicology 37 (5): 496-507. **https://doi. org/10.1177/0960327117714040**.

Ahmed, F. R., M. H. Shoaib, M. Azhar, S. H. Um, R. I. Yousuf, S. Hashmi, and A. Dar. **2015**. "In-Vitro Assessment of Cytotoxicity of Halloysite Nanotubes against HepG2, HCT116 and Human Peripheral Blood Lymphocytes" Colloids and Surfaces. B, Biointerfaces 135: 50-55. **https:// doi.org/10.1016/j.colsurfb.2015.07.021**.

Akintelu, S. A., A. S. Folorunso, F. A. Folorunso, and A. K. Oyebamiji. **2020**. "Green Synthesis of Copper Oxide Nanoparticles for Biomedical Application and Environmental Remediation" Heliyon 6 (7): e04508. **https://doi.org/10.1016/j.heliyon.2020.e04508**.

Arun, J., S. Nachiappan, G. Rangarajan, R. P. Alagappan, K. P. Gopinath, and E. Lichtfouse. **2023**. "Synthesis and Application of Titanium Dioxide Photocatalysis for Energy, Decontamination and Viral Disinfection: A Review" Environmental Chemistry Letters 21 (1): 339-362. **https:// doi.org/10.1007/s10311-022-01503-z**.

Awasthi, S., A. Srivastava, D. Kumar, S. K. Pandey, N. M. Mubarak, M. H. Dehghani, and K. Ansari. **2024**. "An Insight into the Toxicological Impacts of Carbon Nanotubes (CNTs) on Human Health: A Review" Environmental Advances 18: 100601. **https://doi.org/10.1016/j.envadv.2024.100601**.

Baranowska-Wójcik, E., D. Szwajgier, P. Oleszczuk, and A. Winiarska-Mieczan. **2020**. "Effects of Titanium Dioxide Nanoparticles Exposure on Human Health—A Review" Biological Trace Element Research 193 (1): 118-129. **https:// doi.org/10.1007/s12011-019-01706-6**.

Belhadj, J., S. Surina, M. Hengstschläger, and A. J. Lomakin. **2023**. "Form Follows Function: Nuclear Morphology as a Quantifiable Predictor of Cellular Senescence" Aging Cell 22 (12): e14012. **https://doi.org/10.1111/acel.14012**.

Bezza, F. A., S. M. Tichapondwa, and E. M. N. Chirwa. **2020**. "Fabrication of Monodispersed Copper Oxide Nanoparticles with Potential Application as Antimicrobial Agents" Scientific Reports 10 (1): 16680. **https://doi.org/10.1038/s41598-020-73497-z**.

Bo, R., J. Wang, L. Rui, X. Liu, Jiawen Li, Y. Tao, H. Hong, et al. **2023**. "Immunoregulatory Effects on RAW264.7 Cells and Subacute Oral Toxicity of Ultra-Large Pore Mesoporous Silica Nanoparticles Loading Lycium Barbarum Polysaccharides" Journal of Drug Delivery Science and Technology 82: 104192. **https://doi.org/10.1016/j.jddst.2023.104192**.

Brandão, F., N. Fernández-Bertólez, F. Rosário, M. J. Bessa, S. Fraga, E. Pásaro, J. P. Teixeira, B. Laffon, V. Valdiglesias, and C. Costa. **2020**. "Genotoxicity of TiO_2 Nanoparticles in Four Different Human Cell Lines (A549, HEPG2, A172 and SH-SY5Y)" Nanomaterials 10 (3): 412. **https://doi.org/10.3390/nano10030412**.

Brkić Ahmed, L., M. Milić, I. M. Pongrac, A. M. Marjanović, H. Mlinarić, I. Pavičić, S. Gajović, and I. Vinković Vrček. **2017**. "Impact of Surface Functionalization on the Uptake Mechanism and Toxicity Effects of Silver Nanoparticles in HepG2 Cells" Food and Chemical Toxicology 107 (Pt A): 349-361. **https://doi.org/10.1016/j.fct.2017.07.016**.

Bruna, T., F. Maldonado-Bravo, P. Jara, and N. Caro. **2021**. "Silver Nanoparticles and Their Antibacterial Applications." International Journal of Molecular Sciences 22 (13): 7202. **https://doi.org/10.3390/ijms22137202**.

Canta, M., and V. Cauda. **2020**. "The Investigation of the Parameters Affecting the ZnO Nanoparticle Cytotoxicity Behaviour: A Tutorial Review" Biomaterials Science 8 (22): 6157-6174. **https://doi.org/10.1039/D0BM01086C**.

Chairuangkitti, P., S. Lawanprasert, S. Roytrakul, S. Aueviriyavit, D. Phummiratch, K. Kulthong, P. Chanvorachote, and R. Maniratanachote. **2013**. "Silver Nanoparticles Induce Toxicity in A549 Cells via ROS-Dependent and ROS-Independent Pathways." Toxicology in Vitro 27 (1): 330-338. **https://doi.org/10.1016/j.tiv.2012.08.021**.

Chakraborty, N., J. Banerjee, P. Chakraborty, A. Banerjee, S. Chanda, K. Ray, K. Acharya, and J. Sarkar. **2022**. "Green Synthesis of Copper/Copper Oxide Nanoparticles and Their Applications: A Review." Green Chemistry Letters and Reviews. 15 (1): 187-215. **https://doi.org/10.1080/17518253.2022.2025916**.

Chang, Y. N., M. Zhang, L. Xia, J. Zhang, and G. Xing. **2012**. "The Toxic Effects and Mechanisms of CuO and ZnO Nanoparticles" Materials 5 (12): 2850-2871. **https://doi.org/10.3390/ma5122850**.

Chen, P., H. Wang, M. He, B. Chen, B. Yang, and B. Hu. **2019**. "Size-Dependent Cytotoxicity Study of ZnO Nanoparticles in HepG2 Cells." Ecotoxicology and Environmental Safety 171: 337-346. **https://doi.org/10.1016/j.ecoenv.2018.12.096**.

Dussert, F., P.-A. Arthaud, M.-E. Arnal, B. Dalzon, A. Torres, T. Douki, N. Herlin, T. Rabilloud, and M. Carriere. **2020**. "Toxicity to RAW264.7 Macrophages of Silica Nanoparticles and the E551 Food Additive, in Combination with Genotoxic Agents" Nanomaterials 10 (7): 1418. **https://doi.org/10.3390/nano10071418**.

Elje, E., E. Mariussen, O. H. Moriones, N. G. Bastús, V. Puntes, Y. Kohl, M. Dusinska, and E. Rundén-Pran. **2020**. "Hepato(Geno)Toxicity Assessment of Nanoparticles in a HepG2 Liver Spheroid Model" Nanomaterials 10 (3): 545. **https://doi.org/10.3390/nano10030545**.

El-Sayed, R. A., F. M. El-Demerdash, and M. A. El-Magd. **2021**. "Ginseng Ameliorates Pulmonary Toxicity Induced by Silicon Dioxide Nanoparticles in Rats" Asian Pacific Journal of Tropical Biomedicine 11 (6): 254-262

Eskin, A. **2022**. "Effects of Silicon Dioxide Nanoparticles (SiO_2 NPs) on Total Hemocyte Count and Hemocyte Viability of Galleria mellonella" International Journal of Tropical Insect Science 42 (3): 2617-2623. **https://doi.org/10.1007/s42690-022-00790-x**.

Fahmy, B., and S. A. Cormier. **2009**. "Copper Oxide Nanoparticles Induce Oxidative Stress and Cytotoxicity in Airway Epithelial Cells" Toxicology in Vitro 23 (7): 13651371. **https://doi.org/10.1016/j.tiv.2009.08.005**.

Forest, V., L. Leclerc, J.-F. Hochepied, A. Trouvé, G. Sarry, and J. Pourchez. **2017**. "Impact of Cerium Oxide Nanoparticles Shape on Their in Vitro Cellular Toxicity" Toxicology $in\ Vitro$ 38: 136-141. **https://doi.org/10.1016/j.tiv.2016.09.022**.

Fukui, H., M. Horie, S. Endoh, H. Kato, K. Fujita, K. Nishio, L. K. Komaba, et al. **2012**. "Association of Zinc Ion Release and Oxidative Stress Induced by Intratracheal Instillation of ZnO Nanoparticles to Rat Lung" Chemico-Biological Interactions 198 (1-3): 29-37. **https://doi.org/10.1016/j.cbi.2012.04.007**.

Gao, Y., K. Chen, J. Ma, and F. Gao. **2014**. "Cerium Oxide Nanoparticles in Cancer" OncoTargets and Therapy 7: 835840. **https://doi.org/10.2147/OTT.S62057**.

Gao, Y., P. Wen, H. Chen, Y. Wei, H. Cui, J. Ma, J. Li, and G. Qin. **2022**. "Teratogenicity of 30 Nm Aluminum Oxide Nanoparticles (Al_2O_3NPs) in Rats by Gavage" Biological Trace Element Research 200 (9): 4027-4034. **https://doi.org/10.1007/s12011-021-03004-6**.

Giovanni, M., J. Yue, L. Zhang, J. Xie, C. N. Ong, and D. T. Leong. **2015**. "Pro-Inflammatory Responses of RAW264.7 Macrophages When Treated with Ultralow Concentrations of Silver, Titanium Dioxide, and Zinc Oxide Nanoparticles." Journal of Hazardous Materials 297: 146-152. **https://doi.org/10.1016/j.jhazmat.2015.04.081**.

Gudkov, S. V., D. E. Burmistrov, D. A. Serov, M. B. Rebezov, A. A. Semenova, and A. B. Lisitsyn. **2021**. "A Mini Review of Antibacterial Properties of ZnO Nanoparticles." Frontiers in Physics 9:641481.

Guo, X., J.-E. Seo, D. Petibone, V. Tryndyak, U. Lee, T. Zhou, T. Robison, and N. Mei. **2020**. "Performance of HepaRG and HepG2 Cells in the High-Throughput Micronucleus Assay for in Vitro Genotoxicity Assessment." Journal of Toxicology and Environmental Health. Part A 83 (21-22): 702-717. **https://doi.org/10.1080/15287394.2020.1822972**.

Gupta, R., and H. Xie. **2018**. "Nanoparticles in Daily Life: Applications, Toxicity and Regulations" Journal of Environmental Pathology, Toxicology and Oncology 37 (3): 209-230. **https://doi.org/10.1615/JEnvironPatholToxicolOncol.2018026009**.

Gurunathan, S., M. Qasim, C. Park, H. Yoo, J.-H. Kim, and K. Hong. **2018**. "Cytotoxic Potential and Molecular Pathway Analysis of Silver Nanoparticles in Human Colon Cancer Cells HCT116" International Journal of Molecular Sciences 19 (8): 2269. **https://doi.org/10.3390/ijms19082269**.

Hadrup, N., N. Sahlgren, N. R. Jacobsen, A. T. Saber, K. S. Hougaard, U. Vogel, and K. A. Jensen. **2023**. "Toxicity Dose Descriptors from Animal Inhalation Studies of 13 Nanomaterials and Their Bulk and Ionic Counterparts and Variation with Primary Particle Characteristics." Nanotoxicology 17 (4): 338-371. **https://doi.org/10.1080/17435390.2023.2221728**.

Hammond, J., B. A. Maher, T. Gonet, F. Bautista, and D. Allsop. **2022**. "Oxidative Stress, Cytotoxic and Inflammatory Effects of Urban Ultrafine Road-Deposited Dust from the UK and Mexico in Human Epithelial Lung (Calu-3) Cells" Antioxidants 11 (9): 1814. **https://doi.org/10.3390/an-tiox11091814**.

Heinzerling, A., J. Hsu, and F. Yip. **2016**. "Respiratory Health Effects of Ultrafine Particles in Children: A Literature Review" Water, Air, and Soil Pollution 227 (1): 32. **https://doi.org/10.1007/s11270-015-2726-6**.

Helvenstein, M., D. Stanicki, S. Laurent, and B. Blankert. **2015**. "Interaction between Iron Oxide Nanoparticles and HepaRG Cells: A Preliminary in Vitro Evaluation." Journal of Nanomaterials. 2015 (1): 463841. **https://doi.org/10.1155/2015/463841**.

Hsieh, H.-C., C.-M. Chen, W.-Y. Hsieh, C.-Y. Chen, C.-C. Liu, and F.-H. Lin. **2015**. "ROS-Induced Toxicity: exposure of 3T3, RAW264.7, and MCF7 Cells to Superparamagnetic Iron Oxide Nanoparticles Results in Cell Death by Mitochondria-Dependent Apoptosis." Journal of Nanoparticle Research 17 (2): 71. **https://doi.org/10.1007/s11051-015-2886-8**.

Islam, F., S. Shohag, M. J. Uddin, M. R. Islam, M. H. Nafady, A. Akter, S. Mitra, A. Roy, T. Bin Emran, and S. Cavalu. **2022**. "Exploring the Journey of Zinc Oxide Nanoparticles (ZnO-NPs) Toward Biomedical Applications." Materials 15 (6): 2160. **https://doi.org/10.3390/ma15062160**.

Jia, M., W. Zhang, T. He, M. Shu, J. Deng, J. Wang, W. Li, et al. **2020**. "Evaluation of the Genotoxic and Oxidative Damage Potential of Silver Nanoparticles in Human NCM460 and HCT116 Cells" International Journal of Molecular Sciences 21 (5): 1618. **https://doi.org/10.3390/ijms21051618**.

Kim, J.-S., T.-J. Yoon, K.-N. Yu, M. S. Noh, M. Woo, B.-G. Kim, K.-H. Lee, et al. **2006**. "Cellular Uptake of Magnetic Nanoparticle is Mediated through Energy-Dependent Endocytosis in A549 Cells" Journal of Veterinary Science 7 (4): 321-326. **https://doi.org/10.4142/jvs.2006.7.4.321**.

Kolling, A., E. Heinrich, R. Susanne, and U. Heinrich. **2011**. "Relationship of Pulmonary Toxicity and Carcinogenicity of Fine and Ultrafine Granular Dusts in a Rat Bioassay." Inhalation Toxicology 23 (9): 544-554. **https://doi.org/10.3109/08958378.2011.594458**.

Kuhn, J., A. McDonald, C. Mongoin, G. Anderson, G. Lafeuillade, S. Mitchell, A. P D. Elfick, P O. Bagnaninchi, H. H. P Yiu, and L. J. Nelson. **2024**. "Non-Invasive Methods of Monitoring Fe3O4 Magnetic Nanoparticle Toxicity in Human Liver HepaRG Cells Using Impedance Biosensing and Coherent anti-Stokes Raman Spectroscopic (CARS) Microscopy." Toxicology Letters 394: 92-101. **https://doi. org/10.1016/j.toxlet.2024.02.010**.

Kumar, V., N. Sharma, and S. S. Maitra. **2017**. "In Vitro and in Vivo Toxicity Assessment of Nanoparticles" International Nano Letters 7 (4): 243-256. **https://doi.org/10.1007/s40089-017-0221-3**.

Riss TL, Moravec RA, Niles AL, et al. **2013**. Cell Viability Assays. In: Markossian S, Grossman A, Baskir H, et al., editors. Assay Guidance Manual [Internet]. Bethesda (MD): Eli Lilly & Company and the National Center for Advancing Translational Sciences. Available from: **https://www.ncbi. nlm.nih.gov/books/NBK144065/**

Liman, R., Y. Acikbas, İ. H. Ciğerci, M. M. Ali, and M. D. Kars. **2020**. "Cytotoxic and Genotoxic Assessment of Silicon Dioxide Nanoparticles by Allium and Comet Tests" Bulletin of Environmental Contamination and Toxicology 104 (2): 215-221. **https://doi.org/10.1007/s00128-020-02783-3**.

Liu, Y., Z. Zeng, O. Jiang, Y. X. Li, Q. Xu, L. J. Jiang, J. Yu, and D. Xu. **2021**. "Green Synthesis of CuO NPs, Characterization and Their Toxicity Potential against HepG2 Cells." Materials Research Express 8 (1): 015011. **https://doi.org/10.1088/2053-1591/abd666**.

Luceri, A., R. Francese, D. Lembo, M. Ferraris, and C. Balagna. **2023**. "Silver Nanoparticles: Review of Antiviral Properties, Mechanism of Action and Applications." Microorganisms 11 (3): 629. **https://doi.org/10.3390/microorganisms11030629**.

Macko, M., J. Antoš, F. Božek, J. Konečný, J. Huzlík, J. Hegrová, and I. Kuřitka. **2022**. "Development of New Health Risk Assessment of Nanoparticles: EPA Health Risk Assessment Revised" Nanomaterials 13 (1): 20. **https://doi.org/10.3390/nano13010020**.

Marzaioli, V., J. A. Aguilar-Pimentel, I. Weichenmeier, G. Luxenhofer, M. Wiemann, R. Landsiedel, W. Wohlleben, et al. **2014**. "Surface Modifications of Silica Nanoparticles Are Crucial for Their Inert versus Proinflammatory and Immunomodulatory Properties." International Journal of Nanomedicine 9: 2815-2832. **https://doi.org/10.2147/IJN. S57396**.

Mohamed, H. R. H. **2015**. "Estimation of TiO_2 Nanoparticle-Induced Genotoxicity Persistence and Possible Chronic Gastritis-Induction in Mice." Food and Chemical Toxicology 83: 76-83. **https://doi.org/10.1016/j.fct.2015.05.018**.

Mukherjee, R. N., P. Chen, and D. L. Levy. **2016**. "Recent Advances in Understanding Nuclear Size and Shape" Nucleus 7 (2): 167-186. **https://doi.org/10.1080/19491034.2 016.1162933**.

Naika, H. R., K. Lingaraju, K. Manjunath, D. Kumar, G. Nagaraju, D. Suresh, and H. Nagabhushana. **2015**. "Green Synthesis of CuO Nanoparticles Using Gloriosa Superba L. extract and Their Antibacterial Activity." Journal of Taibah University for Science 9 (1): 7-12. **https://doi.org/10.1016/j.jtus-ci.2014.04.006**.

NanoCommons EU Project consortium. "NanoCommons: The European Nanotechnology Knowledge Infrastructure." **2025**. [WWW Document], **https://www.nanocommons.eu/**.

Nayl, A. A., A. I. Abd-Elhamid, A. A. Aly, and S. Bräse. **2022**. "Recent Progress in the Applications of Silica-Based Nanoparticles." RSC Advances 12 (22): 13706-13726. **https://doi.org/10.1039/d2ra01587k**.

Naz, S., A. Gul, and M. Zia. **2020**. "Toxicity of Copper Oxide Nanoparticles: A Review Study" IET Nanobiotechnology 14 (1): 1-13. **https://doi.org/10.1049/iet-nbt.2019.0176**.

Nie, P., Y. Zhao, and H. Xu. **2023**. "Synthesis, Applications, Toxicity and Toxicity Mechanisms of Silver Nanoparticles: A Review." Ecotoxicology and Environmental Safety 253: 114636. **https://doi.org/10.1016/j.ecoenv.2023.114636**.

Nosaka, Y., and A. Y. Nosaka. **2017**. "Generation and Detection of Reactive Oxygen Species in Photocatalysis" Chemical Reviews 117 (17): 11302-11336. **https://doi.org/10.1021/acs.chemrev.7b00161**.

Ophir, N., A. Bar Shai, R. Korenstein, M. R. Kramer, and E. Fireman. **2019**. "Functional, Inflammatory and Interstitial Impairment Due to Artificial Stone Dust Ultrafine Particles Exposure" Occupational and Environmental Medicine 76 (12): 875-879. **https://doi.org/10.1136/oemed-2019-105711**.

Pansambal, S., R. Oza, S. Borgave, A. Chauhan, P. Bardapurkar, S. Vyas, and S. Ghotekar. **2023**. "Bioengineered Cerium Oxide (CeO_2) Nanoparticles and Their Diverse Applications: A Review" Applied Nanoscience 13 (9): 6067-6092. **https://doi.org/10.1007/s13204-022-02574-8**.

Park, E.-J., G.-H. Lee, C. Yoon, U. Jeong, Y. Kim, M.-H. Cho, and D.-W. Kim. **2016**. "Biodistribution and Toxicity of Spherical Aluminum Oxide Nanoparticles" Journal of Applied Toxicology 36 (3): 424-433. **https://doi.org/10.1002/jat.3233**.

Park, E.-J., J. Sim, Y. Kim, B. S. Han, C. Yoon, S. Lee, M.-H. Cho, B.-S. Lee, and J.-H. Kim. **2015**. "A 13-Week Repeated-Dose Oral Toxicity and Bioaccumulation of Aluminum Oxide Nanoparticles in Mice." Archives of Toxicology 89 (3): 371379. **https://doi.org/10.1007/s00204-014-1256-0**.

Rafieepour, A., M. R. Azari, F. Khodagholi, J. P. Jaktaji, Y. Mehrabi, and H. Peirovi. **2021**. "Interactive Toxicity Effect of Combined Exposure to Hematite and Amorphous Silicon Dioxide Nanoparticles in Human A549 Cell Line" Toxicology and Industrial Health 37 (5): 289-302. **https://doi. org/10.1177/07482337211002373**.

Rafieepour, A., M. R. Azari, and F. Khodagholi. **2023**. "Cytotoxic Effects of Crystalline Silica in Form of Micro and Nanoparticles on the Human Lung Cell Line A549" Toxicology and Industrial Health 39 (1): 23-35. **https://doi. org/10.1177/07482337221140644**.

Reihani, A., F. Shaki, and A. Azari. **2025**. "Zinc Oxide Nanoparticles Decrease Acrylamide Cytotoxicity and Oxidative Stress in HepG2 Cells" Nutrition & Food Science 55 (3): 481-492. **https://doi.org/10.1108/NFS-07-2023-0147**.

Samuel, M. S., M. Ravikumar, A. John, J. E. Selvarajan, H. Patel, P. S. Chander, J. Soundarya, S. Vuppala, R. Ba laji, and N. Chandrasekar. **2022**. "A Review on Green Synthesis of Nanoparticles and Their Diverse Biomedical and Environmental Applications." Catalysts 12 (5): 459. **https://doi.org/10.3390/catal12050459**.

Savage, D. T., J. Z. Hilt, and T. D. Dziubla. **2019**. "In Vitro Methods for Assessing Nanoparticle Toxicity" In: Zhang, Q. (eds) Nanotoxicity. Methods in Molecular Biology, (1894): 1-29. Humana Press Inc., NY

Silva, B. L. da., M. P. Abuçafy, E. B. Manaia, J. A. O. Junior, B. G. Chiari-Andréo, R. C. L. R. Pietro, and L. A. Chiavacci. **2019**. "Relationship between Structure and Antimicrobial Activity of Zinc Oxide Nanoparticles: An Overview." International Journal of Nanomedicine 14: 9395-9410. **https://doi.org/10.2147/IJN.S216204**.

Singh, A. V., M. Varma, P. Laux, S. Choudhary, A. K. Datusalia, N. Gupta, A. Luch, A. Gandhi, P. Kulkarni, and B. Nath. **2023**. "Artificial Intelligence and Machine Learning Disciplines with the Potential to Improve the Nanotoxicology and Nanomedicine Fields: A Comprehensive Review" Archives of Toxicology 97 (4): 963-979. **https://doi.org/10.1007/s00204-023-03471-x**.

Singh, K. R. B., V. Nayak, T. Sarkar, and R. P. Singh. **2020**. "Cerium Oxide Nanoparticles: Properties, Biosynthesis and Biomedical Application" RSC Advances 10 (45): 2719427214. **https://doi.org/10.1039/d0ra04736h**.

Single, A., H. Beetham, B. J. Telford, P. Guilford, and A. Chen. **2015**. "A Comparison of Real-Time and Endpoint Cell Viability Assays for Improved Synthetic Lethal Drug Validation" Journal of Biomolecular Screening 20 (10): 12861293. **https://doi.org/10.1177/1087057115605765**.

Slowing, I. I., J. L. Vivero-Escoto, C.-W. Wu, and V. S.-Y. Lin. **2008**. "Mesoporous Silica Nanoparticles as Controlled Release Drug Delivery and Gene Transfection Carriers." Advanced Drug Delivery Reviews 60 (11): 1278-1288. **https://doi.org/10.1016/j.addr.2008.03.012**.

Song, W., J. Zhang, J. Guo, J. Zhang, F. Ding, L. Li, and Z. Sun. **2010**. "Role of the Dissolved Zinc Ion and Reactive Oxygen Species in Cytotoxicity of ZnO Nanoparticles." Toxicology Letters 199 (3): 389-397. **https://doi.org/10.1016/j.toxlet.2010.10.003**.

Strigul, N., L. Vaccari, C. Galdun, M. Wazne, X. Liu, C. Christodoulatos, and K. Jasinkiewicz. **2009**. "Acute Toxicity of Boron, Titanium Dioxide, and Aluminum Nanoparticles to Daphnia Magna and Vibrio fischeri" Desalination 248 (1-3): 771-782. **https://doi.org/10.1016/j.desal.2009.01.013**.

Thakur, N., N. Thakur, A. Kumar, V. K. Thakur, S. Kalia, V. Arya, A. Kumar, S. Kumar, and G. Z. Kyzas. **2024**. "A Critical Review on the Recent Trends of Photocatalytic, Antibacterial, Antioxidant and Nanohybrid Applications of Anatase and Rutile TiO_2 Nanoparticles." The Science of the Total Environment 914: 169815. **https://doi.org/10.1016/j.scitotenv.2023.169815**.

Uo, M., T. Akasaka, F. Watari, Y. Sato, and K. Tohji. **2011**. "Toxicity Evaluations of Various Carbon Nanomaterials" Dental Materials Journal 30 (3): 245-263. **https://doi.org/10.4012/dmj.2010-039**.

Vecchiotti, G., S. Colafarina, M. Aloisi, O. Zarivi, P. Di Carlo, and A. Poma. **2021**. "Genotoxicity and Oxidative Stress Induction by Polystyrene Nanoparticles in the Colorectal Cancer Cell Line HCT116" PLOS One 16 (7): e0255120. **https://doi.org/10.1371/journal.pone.0255120**.

Vijayaraghavareddy, P, V. Adhinarayanreddy, R. S. Vemanna, S. Sreeman, and U. Makarla. **2017**. "Quantification of Membrane Damage/Cell Death Using Evan's Blue Staining Technique" Bioprotocol 7 (16): e2519. **https://doi.org/10.21769/bioprotoc.2519**.

Voss, L., K. Yilmaz, L. Burkard, J. Vidmar, V. Stock, U. Hoffmann, O. Pötz, et al. **2020**. "Impact of Iron Oxide Nanoparticles on Xenobiotic Metabolism in HepaRG Cells" Archives of Toxicology 94 (12): 4023-4035. **https://doi.org/10.1007/s00204-020-02904-1**.

Xu, L., Y. Y. Wang, J. Huang, C. Y. Chen, Z. X. Wang, and H. Xie. **2020**. "Silver Nanoparticles: Synthesis, Medical Applications and Biosafety" Theranostics 10 (20): 8996-9031. **https://doi. org/10.7150/thno.45413**.

Yang, S. A., S. Choi, S. M. Jeon, and J. Yu. **2018**. "Silica Nanoparticle Stability in Biological Media Revisited." Scientific Reports 8 (1): 185. **https://doi.org/10.1038/s41598-017-18502-8**.

Yang, Y., X. Du, Q. Wang, J. Liu, E. Zhang, L. Sai, C. Peng, et al. **2019**. "Mechanism of Cell Death Induced by Silica Nanoparticles in Hepatocyte Cells is by Apoptosis" International Journal of Molecular Medicine 44 (3): 903-912. **https://doi.org/10.3892/ijmm.2019.4265**.

Yip, S. K., and J. A. Sauls. **1992**. "Nonlinear Meissner Effect in CuO Superconductors" Physical Review Letters 69 (15): 2264-2267. **https://doi.org/10.1103/PhysRevLett.69.2264**.

Yuan, Y., C. Liu, J. Lu, W. Tang, Q. Gan, H. Zhou, J. Qian, and X. Lu. **2011**. "In Vitro Cytotoxicity and Induction of Apoptosis by Silica Nanoparticles in Human HepG2 Hepatoma Cells." International Journal of Nanomedicine 6: 1889-1901. **https://doi.org/10.2147/ijn.s24005**.

Ziental, D., B. Czarczynska-Goslinska, D. T. Mlynarczyk, A. Glowacka-Sobotta, B. Stanisz, T. Goslinski, and L. Sobotta. **2020**. "Titanium Dioxide Nanoparticles: Prospects and Applications in Medicine" Nanomaterials 10 (2): 387. **https://doi.org/10.3390/nano10020387**.

Zorova, L. D., V. A. Popkov, E. J. Plotnikov, D. N. Silachev, I. B. Pevzner, S. S. Jankauskas, S. D. Zorov, V. A. Babenko, and D. B. Zorov. **2018**. "Functional Significance of the Mitochondrial Membrane Potential" Biochemistry, Supplement Series A: Membrane and Cell Biology 12 (1): 20-26. **https://doi. org/10.1134/S1990747818010129**.